iScience

Article

MemorySeq identifies heritable epigenetic phenotypes that initiate cell culture stress tolerance in CHO cells

Graphical abstract

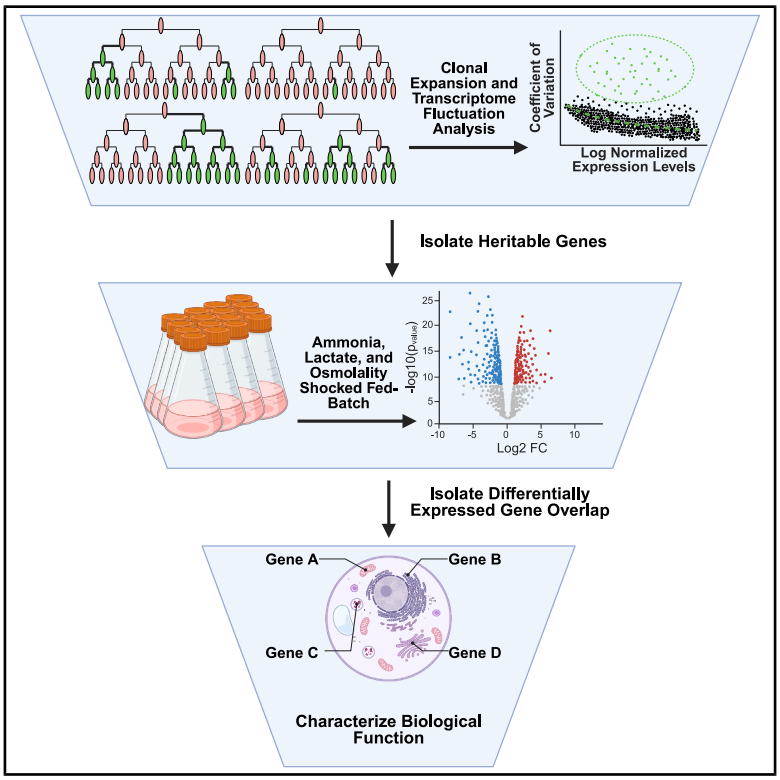

Authors

Spencer Grissom, Zachary Dixon, Abhyudai Singh, Mark Blenner

Correspondence

blenner@udel.edu

In brief

Cell engineering; Epigenetics; Expression study; Flux data; Transcriptomics

Highlights

- Traditional transcriptomics often yield ambiguous and difficult-to-interpret results
- An alternative in MemorySeq quantifies heritability in intermediate timescales
- Heritable gene states are enriched in anti-apoptotic and pro-proliferative genes
- Stress shocked cells are enriched in these heritable gene states

Grissom et al., 2025, iScience *28*, 113478
October 17, 2025
https://doi.org/10.1016/j.isci.2025.113478

CellPress

iScience

CellPress
OPEN ACCESS

Article

MemorySeq identifies heritable epigenetic phenotypes that initiate cell culture stress tolerance in CHO cells

Spencer Grissom,[1] Zachary Dixon,[1] Abhyudai Singh,[2] and Mark Blenner[1,3,*]
[1]Chemical & Biomolecular Engineering, University of Delaware, Newark, DE 19713, USA
[2]Electrical and Computer Engineering, University of Delaware, Newark, DE 19713, USA
[3]Lead contact
*Correspondence: blenner@udel.edu
https://doi.org/10.1016/j.isci.2025.113478

SUMMARY

During manufacturing batches, Chinese hamster ovary (CHO) cells encounter critical levels of environmental stressors which can significantly reduce cell health and productivity. Therefore, stress tolerance must be considered during selection of a suitable host. In this study, we employ a population-based transcriptomic method, referred to as MemorySeq, and differential gene expression analysis on stress-shocked CHO cells to identify stress responsive biomarkers. These biomarkers exhibit transient and intermediate heritable memory states characteristic of epigenetic switches and transcriptional bursting. Using this workflow, 199 genes were found to exhibit transcriptional variability characteristic of two-state systems with switching that forms four network communities of co-fluctuating genes. These communities were enriched in genes related to the regulation of apoptotic processes, gene expression, and metabolic pathways. Seven genes were identified as promising biomarkers of stress-resistance. Genetic engineering methods may be employed in the future to bias clonal populations toward higher stress tolerance to manufacturing stress.

INTRODUCTION

Mammalian cells, in particular Chinese hamster ovary (CHO) cells, are favored for monoclonal antibody (mAb) production due to their favorable growth properties, rapid adaptability, and human-like post-translational modifications (PTMs).[1,2] Like many immortalized cell lines, CHO cells are also characterized by transcriptional plasticity that leads to genetic drift, instability, and subclonal heterogeneity.[3,4] While this plasticity is partly due to genomic instability, a frequently overlooked contributor is the dynamic epigenome. Epigenetic heterogeneity is driven by post-translational modifications to the DNA, RNA, histone proteins, and regulation by non-coding regulatory RNA.[5,6] These epigenetic effects commonly produce rapid transient changes, and also produce rare longer transient changes that persist beyond a cell generation creating heritable ''memory states''.[7] The relationship between epigenetic marks and gene expression has been demonstrated in CHO cells through the formation of distinct chromatin states characterized by unique histone modifications and DNA methylation patterns in response to variable culture conditions.[8–10] Epigenetic regulation offers speed and reversibility compared to genetic mutations with transgenerational lifetimes anywhere from weeks in the case of DNA methylation to days for histone acetylation.[11,12]

These modifications result in distinct phenotypes characterized by multiple transient semi-stable levels of gene expression that are inherited from parent to progeny. These rare expression patterns have been identified in several organisms and the lifetime varies on whether the system is truly epigenetically maintained and forms a metastable state or is the consequence of transient coordinated fluctuations.[13–15] These heritable gene states described previouslycharacterize a phenomenon referred to as an epigenetic switch that permits the transition between various expression levels.[16] Genes or gene networks with heritable epigenetic states promote phenotypic diversity and plasticity to permit rapid adaptation to environmental stress within a subset of the population that can be inherited.[17,18] Stress-resistance genes impose a metabolic burden when the stressor is absent, reducing growth, and fitness.[19] When an environmental stressor is encountered, the presence of metastable systems formed from epigenetic diversity promotes the survival of stress-tolerant subpopulations and appears faster compared to the sluggish pace required for a favorable genetic mutation to appear. The premise of phenotypic plasticity and transcriptional bursting has been observed across various cancer cells where differential epigenetic regulation of genes, such as *MDR1/ABCB1* or *EGFR* enables drug-resistant cells to persist even without drug exposure.[15,20,21]

During at-scale production, CHO cells encounter many perturbations to their environment, such as the accumulation of toxic metabolic byproducts, shear during sparging and mixing, high osmolality during pH maintenance, and significant spatial and temporal heterogeneity.[22–26] These stresses can reduce specific cell growth rates, reduce productivity, and influence N-linked

glycosylation patterns.[22,27–29] While many studies into stress response pathways only consider phenotypic changes and differentially expressed genes (DEGs), they do not indicate which genes are responsible for stress adaptation and tolerance nor which genes initiate the response.[22,27,30,31] Alternative methods are required to interpret the noise of traditional transcriptomic tools in order to develop an understanding of the regulatory gene networks that contribute to heritable stress tolerant phenotypes and suggest engineering targets to improve CHO cell line performance.

An elegant experimental method known as MemorySeq was developed by Shaffer et al. for the purpose of identifying these heritable gene expression states.[32] This technique is reminiscent of the classical Luria-Delbrück experiment to investigate whether bacteriophage resistance developed because of selective pressure or from random fluctuations of a resistant phenotype during cell-division.[33] That work, known as the fluctuation test, showed the development of a phage resistant phenotype occurred spontaneously in the absence of selective pressure and was inherited by progeny. This phenomenon has been observed in other organisms such as *Priestia megaterium* developing antibiotic resistance or lung epithelial cells with differential susceptibility to adenovirus.[34,35] MemorySeq similarly explores gene expression states that spontaneously arise and are inherited by progeny by closely monitoring the transcriptomic profile of single cell-derived clonal populations, which represents intermediate cellular memory states.

This project seeks to address this gap in knowledge through the identification of heritable biomarkers that could be selected or engineered in a rational design approach to yield a stress-tolerant phenotype. Biomarkers are a gene expression pattern that confers a distinct phenotype and are often identified using transcriptomic, proteomic, and/or metabolomic profiling.[36] Using MemorySeq, nearly 200 genes demonstrating intermediate heritability were identified and their complex interactions were explored. When compared to DEGs caused by CHO cell manufacturing stresses, we found these heritable gene networks are significantly enriched in stress response genes characterized by regulation of the cell cycle, apoptotic processes, and stimuli detection. The intersection of DEGs observed in stressful media to unstressed MemorySeq heritability data enabled identification of genes that may play a role in the initiation of stress tolerance phenotypes.

RESULTS

MemorySeq identifies heritable gene expression states in CHO cells

The MemorySeq workflow, originally developed by Shaffer et al., was intended to identify a panel of genes associated with rare pre-drug resistance phenotypes that persisted for several generations in cancer cells.[32] In this method, they posited that some rare phenotypes can be simplified as a two-state system, in which sparse cells exist in an aberrant state, referred to as the "On" state that is characterized by an uncharacteristically "high" or "low" expression level for a specific gene. In contrast, cells that are in the "Off" state, represent the most abundant expression state for a given gene. The prevalence of the rare phenotype has been demonstrated in other cell lines, such as WM989 cells, to occur within roughly 1%–2% of cells using small-molecule RNA fluorescence *in-situ* hybridization (smRNA-FISH) and flow cytometry.[32] A slow rate of transitioning to the "On" state paired with a high probability of inheriting the "On" state characterizes a heritable gene expression state. Fluctuations between the "On" state and the "Off" state that are rapid and stochastic with no correlation between progeny and parent cell characterize non-heritable gene expression states. In other words, if the lifetime of the "On" expression state is significantly longer than the characteristic time for cell-division, the rare phenotype will persist across multiple generations and be enriched in the progeny (Figure 1A). Importantly, it would prove difficult to differentiate these two patterns using scRNA-seq as it requires tracking population dynamics and tracing common lineages between cells. Once the cells have grown for many generations, the appearance of rare phenotypes is indistinguishable between natural biological noise or the shift to a stable and heritable phenotype (Figure S1).

In MemorySeq, around 40 single-cell populations of the CHOZN GS$^{-/-}$ Clone 23 strain were seeded using limited dilution cloning (LDC) techniques to form the MemorySeq clones. These monoclonal populations were expanded until there were roughly 100,000 cells, reflecting 16–17 generations of growth over 3–4 weeks. This method seeks to capture the intermediate timescales in which rare phenotypes may first appear by constraining growth to the first 17 generations (achieving about 100,000 cells) and observe as the phenotype gradually becomes more prevalent in the broader population. The fluctuations that appear in pools with fewer cells would eventually reach a point of equilibrium if expanded well beyond 17 generations, limiting the ability to monitor and measure appearance of transient phenotypes. At this time, the whole RNA content of the MemorySeq clones was extracted and sequenced. Alongside these samples, 40 RNA samples collected from 100,000 bulk cells in a standard passage flask constituted the noise control, where there is no shared lineage in the resulting population. The noise control represents natural biological variability and what the expression would appear for a clone grown many generations. For protein-coding genes, there are two expected distributions of gene expression. The first is a roughly normal distribution centered near the noise control average and reflects non-heritable expression states as the rapid fluctuations maintain a roughly constant number of high expressing clones. This distribution displays relatively low variability in expression. The other is typically a positive or negative-skew distribution characterized by high variance with an elongated tail. The variance and skew are explained by the lineage-dependent expression level as the generation at which a parent cell first transitions into the rare, "On" expression state influences the final expression level of the progeny. If the transition occurs earlier, then the final population would be enriched in the rare phenotype and be skewed relative to a MemorySeq sample that transitioned late or never transitioned at all (Figure 1B). Noise control samples are expected to be tightly distributed as there is no common lineage between cells in the sample and bulk expression is biased toward the average expression level.

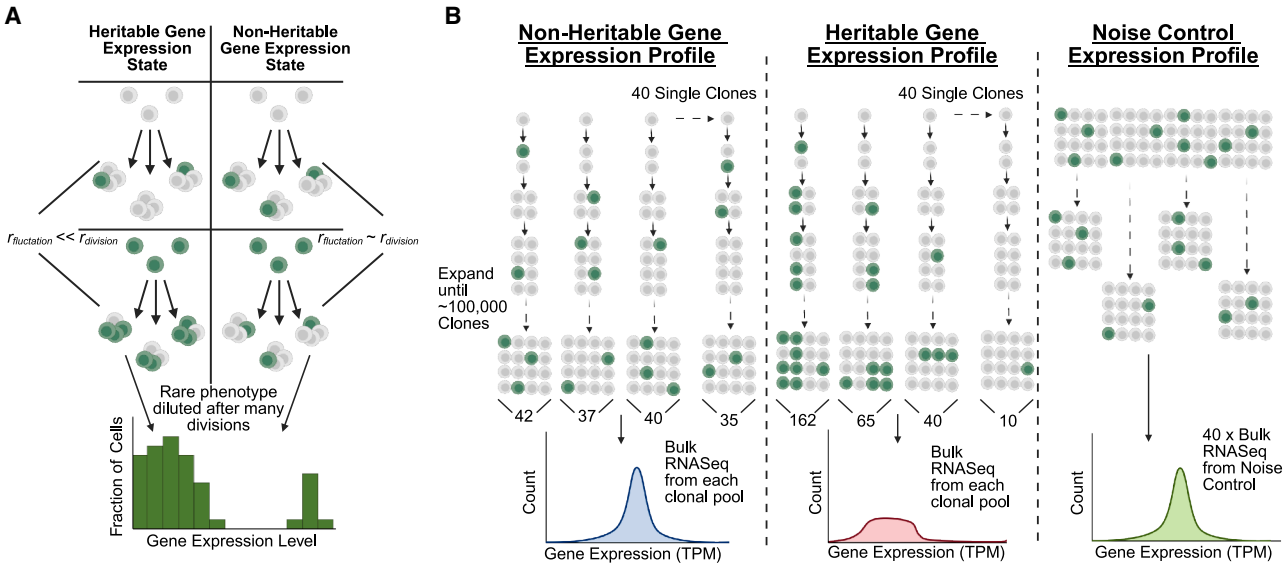

Figure 1. Summary of MemorySeq workflow and fluctuation analysis for identifying heritable gene states: Graphical principles for MemorySeq workflow

(A) Summary of heritable gene expression patterns for rare phenotypes. In this simplified model, green cells exhibit the rare-cell gene expression pattern and are surmised to be "On" while the white cells exhibit a bulk, lower average expression level and are said to be "Off".

(B) MemorySeq workflow and basis for identifying heritable gene expression states. Starting from a bulk CHOZN GS$^{-/-}$ Clone 23 passage flask, LDC techniques were used to seed sufficient wells to acquire $n = 40$ single-cell clones. Comparison of bulk RNA-seq samples between monoclonal derived cell pools and those from a bulk population forms the basis for how heritable genes are identified as heritable genes form a non-Gaussian expression distribution while non-heritable genes do not.

MemorySeq identifies 199 heritable gene states in CHO cells

After all RNA samples were collected and submitted for sequencing, there were 38 MemorySeq samples and 40 noise control samples left after quality control. Of the 32,428 initial gene counts measured, only protein-coding genes with a minimum expression level of 2.5 transcripts per million (TPM) were included in the analysis as low expressing genes display greater variability that may skew downstream analysis.[32] Metrics of variation were calculated for the remaining 10,106 genes. Heritability is marked by significantly greater variability and skew, which is directly related to when the rare phenotype first appears compared to rapidly fluctuating non-heritable gene states (Figures S2A and S2B). A gene displaying no tendency to inherit a rare expression state would possess a roughly 1:1 ratio of the coefficient of variation (CV) between the MemorySeq samples and the noise control. The overall variance observed in MemorySeq clones however were innately higher than the noise control samples due to the bias of cell-to-cell variability, yielding a ratio of $\frac{CV_{MemorySeq\ Clones}}{CV_{Noise\ Control}}$ greater than unity for a majority of the genes (Figure 2A). A comparison of the 95% confidence intervals from 10,000 samples generated from bootstrapping revealed that a majority of the CVs were statistically greater in MemorySeq samples with a p value less than 0.001 (Figure S2C). An alternative approach for identifying genetic states with heritable properties involves fitting a Poisson regression between the coefficient of variation in TPM and the $\log_2(\text{Mean}_{TPM})$[37,38] (Figure 2B). Genes that deviate significantly from the fit are those that have a statistically high variance for its corresponding expression level. Related to this is the theory that CV monotonically increases with the duration a cell occupies a rare phenotype.[15] Therefore, genes with the slowest rate of fluctuation are those with the greatest variation. To identify the genes with heritable expression states, piecewise linear regression was used to identify the breakpoint at which the residuals significantly deviated (Figure S2D). A range between the 98th and 95th percentile captured this breakpoint well, where 98th percentile was chosen to isolate only the most slowly fluctuating genes. There were 15 genes within the noise control that exceeded the residual threshold and the single redundancy within the MemorySeq clones was removed as the natural variability of this gene confounds variability due to principles of heritability. Residuals were compared to the critical threshold and 199 heritable gene states were identified. These genes appeared to be spread out in clusters across all 21 chromosomes with some common regulation patterns (Figure S3) and displayed the characteristic "smear" or positive skew distribution in MemorySeq clones expected for heritable genes compared to the narrow and low variation noise control (Figure 2C). It is important to note that *a priori* knowledge regarding the frequency of a given rare phenotype is not required nor assumed in identifying genes displaying prolonged inheritance.

Epigenomic and transcriptional characterization of heritable gene states highlights key deviations

The observed transcriptional fluctuations would possibly suggest that heritability coincides with poised or bivalent chromatin states. These chromatin states are marked by histone or DNA

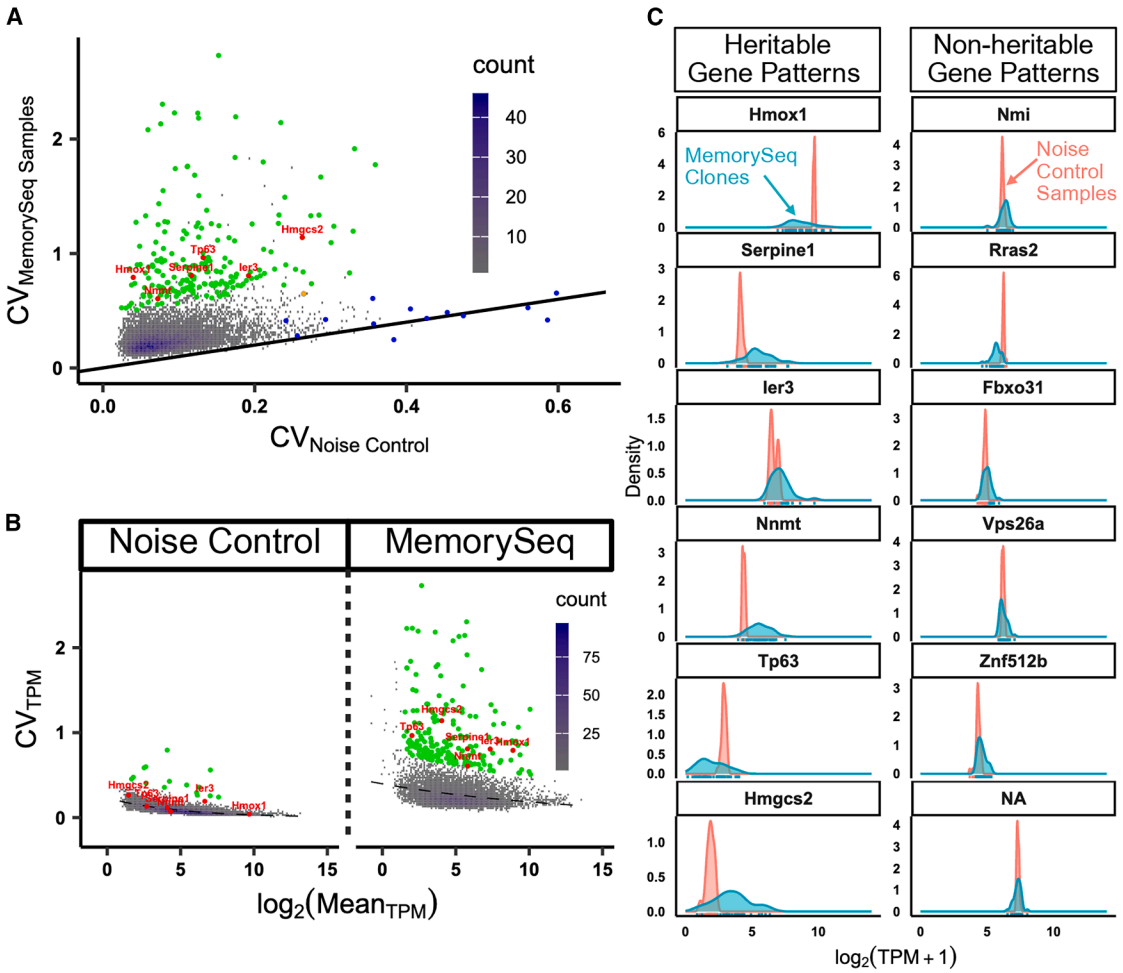

Figure 2. Application of MemorySeq identifies 199 heritable gene states in CHO cells: Visualization of heritable and non-heritable gene expression states

(A) Coefficient of variation for TPM for MemorySeq Samples versus noise control. Each dot represents one of 10,106 different genes or a cluster of genes in which the color corresponds to the density of genes in each bin. Green dots represent those genes in the top 2% of residuals from the Poisson regression fit from the MemorySeq Samples while the blue dots are those in the top 2% of residuals from the noise control. The lone orange dot represents the one gene that was in the top 2% of residuals of both populations.

(B) Coefficient of variation for transcripts per million versus log normalized average transcripts per million for noise control and MemorySeq samples. Each dot represents a different gene or cluster of genes. Upon fitting a Poisson regression distribution to each group, visualized as the dashed line, the genes that were in the top 2% of residuals and had an average $\log_2$(TPM) of 2.5 or greater are highlighted as green and considered to have a heritable gene expression profile. Any overlapping genes that were in the top 2% residuals and in the noise control were removed from consideration due to inherit biological noise. Genes of interest, to be discussed later, are marked in red.

(C) Sample histograms for gene expression for six heritable (Left) and six non-heritable (Right) gene expression patterns. The blue curve corresponds to the distribution of MemorySeq clone expression and the pink is the distribution of noise control expression.

methylation patterns that are both activating and repressive and give rise to greater phenotypic plasticity such that a transition to a distinct phenotype is simplified by small disturbances to the local epigenetic state.[39,40] To investigate whether there are conserved epigenetic features of the genes displaying heritable characteristics, historical DNA methylation from bisulfite sequencing and histone marks from chromatin immunoprecipitation (ChIP) sequencing datasets published by Feichtinger et al. were aligned to the PICR genome.[8] These datasets were generated using high producing CHO-K1 cells, a close analog to the cells used in this work. DNA methylation of the promoter region upstream of the transcription start site (TSS) is predominantly a repressive and transgenerational mark. The regions contain a high concentration of CpG islands or CG dinucleotides vulnerable to DNA methylation (Figure 3A). Many developmental genes become hypermethylated while essential genes remain hypomethylated. Intermediate methylation levels are an indicator of a poised state and a conserved signature of gene regulation as there is a lower barrier to transitioning toward hypo or hypermethylation states.[41,42] The average expression in the MemorySeq samples for the heritable gene pool (87.2 TPM) was lower than the non-heritable gene pool (98.8 TPM). The rates

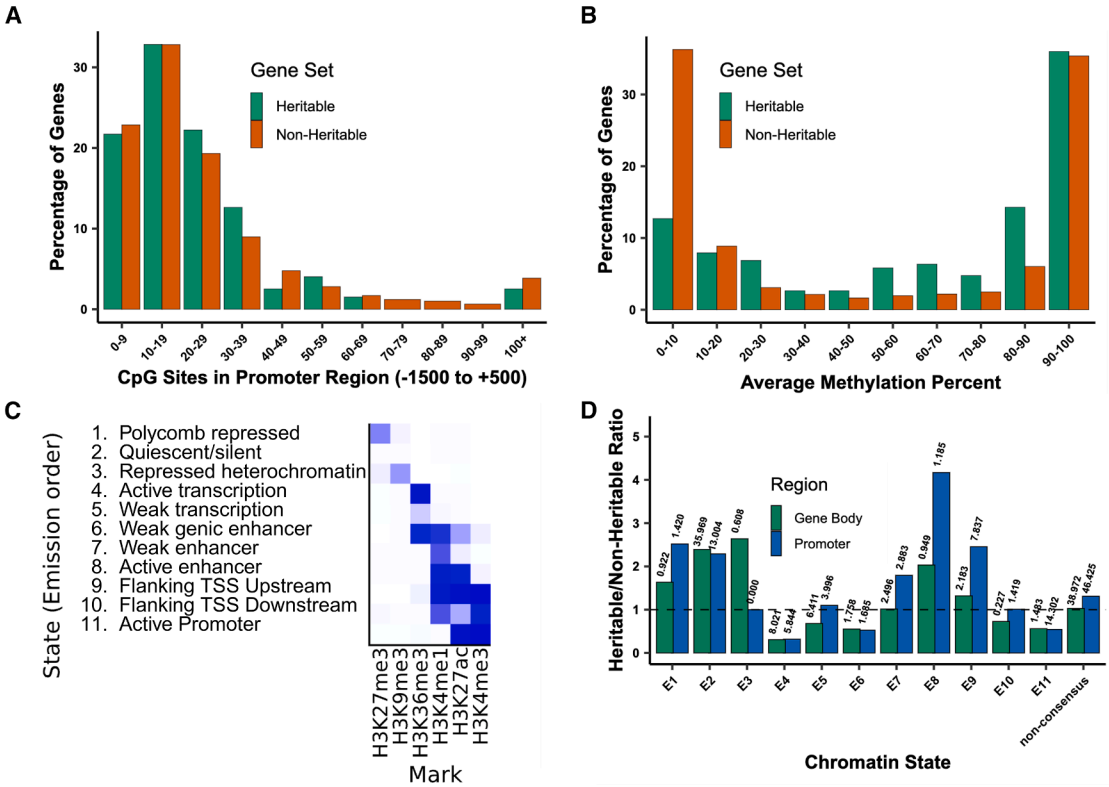

Figure 3. Epigenomic characterization of heritable gene promoter and gene body regions

(A) CpG island density within the −1,500 to +500 bp promoter region relative to the TSS for both heritable and non-heritable gene sets.

(B) Distribution of methylation patterns across heritable and non-heritable gene sets. Promoter regions with less than six CpG islands and CpG islands with less than a coverage of four were filtered out. Hypomethylated regions defined as promoters with 0%–10% while hypermethylated defined as those with 90%–100% methylation.

(C) Eleven chromatin states defined by ChromHMM using six histone marks to define model.

(D) Relative ratios of chromatin state occupancy for heritable and non-heritable gene sets within either gene body or promoter regions. Ratios greater than unity defines enrichment and percentages shown represent the heritable gene set occupancy.

of DNA hypermethylation (90%–100%) were nearly identical between the two gene sets across the promoter region defined as the −1500 to +500 bp region relative to the TSS.[43] However, the rate of intermediate methylation (20%–80%) was more than doubled in the heritable gene pool at 29.1% compared to 13.5% (Figure 3B). The average methylation for the heritable gene pool was significantly higher than the non-heritable gene pool (Wilcoxon rank-sum test p value <0.01). This prevalence of intermediate methylation patterns may suggest one mechanism by which these highly variable genes undergo transcriptional fluctuation during short timescales.

Another feature to consider is the concentration and combination of histone marks that outline distinct regulatory functions and chromatin states. Using the Feichtinger et al. ChIP-Seq consensus data across three time points to train a hidden Markov model (HMM) model, eleven unique chromatin states were identified and aligned to the two gene pools (Figure 3C). Across both the gene body and the promoter region, heritable genes had 1.6 to 2.7-fold greater occupancy by repressed, quiescent, and heterochromatin relative to non-heritable genes, and lower occupancy in active transcriptional states (Figure 3D). Furthermore, genes with intermediate heritability were 4.2 times more likely to have greater occupancy of active enhancer states in the promoter region. This contrast of repressive histone marks, but proximity to active enhancers further outlines the bivalent epigenetic traits of the genes displaying heritable properties.

To verify the heritability principles for some of the physiologically relevant genes identified as heritable, smRNA-FISH was completed for *Hmox1* and *Ier3*. These genes were chosen as they had the highest basal expression, making signal intensity easiest to capture among the seven genes of interest (discussed more later). To measure the shared lineage across multiple cell-divisions, cells were first attached to a fibronectin-coated coverglass to promote cellular adhesion and grown to 60%–70% confluence. In doing so, the proximity of cells with respect to one another is good approximation for their relatedness or common lineage. As cells begin to transition to the high expression state, they serve as a nucleus for a larger, contiguous population of highly expressing cells if they are heritable (Figure S4). This pattern of outgrowth can be captured visually by hybridization to fluorescently labeled RNA probes corresponding to some of the heritable genes of interest.[32] Highly expressing cells were

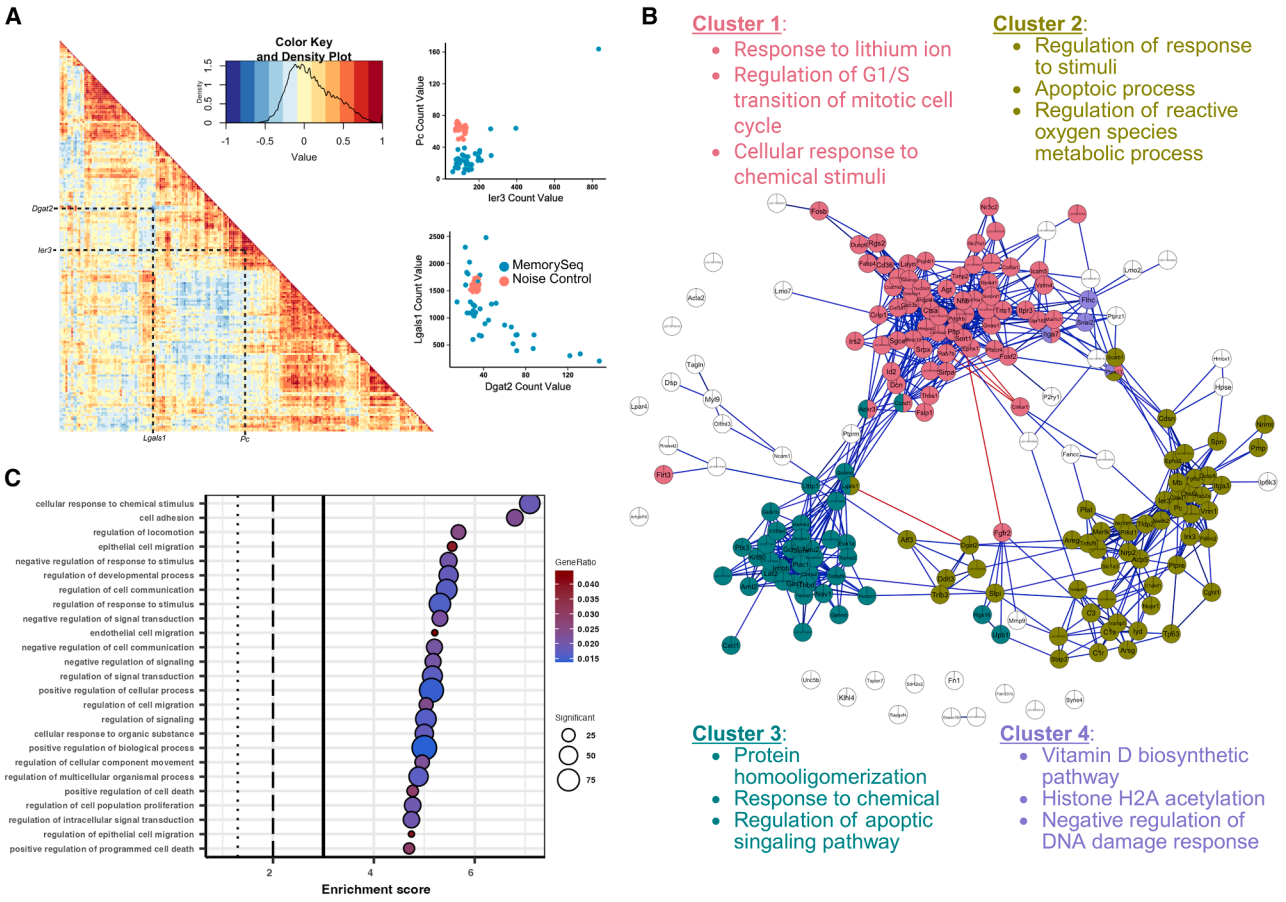

Figure 4. Network community identification of heritable gene states reveals four co-fluctuating communities with shared biological processes

(A) Pearson pairwise correlation matrix for all 199 heritable gene states to highlight expression co-fluctuations between gene pairs. Red or positive correlations signify the mutual increase in expression levels between a gene pair (Example between Pc and Cited1 shown in bottom right). Blue or negative correlations signify the reduced expression of one gene coinciding with the enhanced expression of another gene (Example between Lgals1 and Dgat2 shown in top right).

(B) Product of k-clique percolation for network community identification of the 199 heritable gene states for $k = 4$ and $l = 0.68$. Four distinct communities identified, differentiated by different colors along with GO terms enriched within the individual communities. Unlinked genes are shown in white and did not meet the k−1 requirement for inclusion within other networks.

(C) Dot plot visualizing the 25 most enriched GO terms across all 199 heritable gene states. Size and color intensity reflect the number of genes contained with each GO term and the corresponding gene ratio. Dotted lines represent a *p*-value of 0.05, 0.01, and 0.001 from left to right.

rare in the bulk population, but several pockets of such cells were observed for *Hmox1* and *Ier3*.

Network community identification of heritable gene states reveals four co-fluctuating communities with shared biological processes

Complex phenotypes are rarely the result of a single gene, but rather the simultaneous co-expression of network communities. To further elucidate the relationships between the 199 heritable gene expressions states, a Pearson correlation coefficient was calculated between all pairwise comparisons (Figure 4A). A plurality of genes exhibited a strongly positive correlation, indicating a co-regulation that activates gene expression. To investigate how sensitive these correlations were to outliers, the Cook's distance of strongly correlated pairs was measured to determine if any biological replicate consistently skewed the correlations. Some outliers are implicitly expected in the data as an early transition to the rare "high" expression state yields a heavily skewed distribution. However, if an outlier is considerably larger or smaller than the average, it suppresses the variability captured in the remaining MemorySeq clones and dominates the magnitude of the variance and correlation. This can shift a gene that otherwise appears non-heritable to a heritable classification. The origin of the outlier can stem from an unusually early transition or may result from genetic drift into a unique phenotype. CHO is particularly vulnerable to genetic drift due to genomic instability, but drift is random and still yields roughly normally distributed gene expression profiles.[44] This stochastic phenomenon contributes to cell-to-cell variability and may produce outliers, but does not explain the consistent and coordinated fluctuations observed here.[45] Pool 2 of the MemorySeq clonally derived samples was identified as a consistent outlier in Cook's

distance analysis and was removed from the dataset to yield 37 MemorySeq replicates and 40 noise control replicates (Figure S5).

Network community identification from the correlations of pairwise co-fluctuating genes was carried out through a *k*-clique percolation method (*k*-CPM). The output of *k*-CPM is the identification of overlapping network communities of strongly co-fluctuating gene expression states that may outline a unique phenotype.[46,47] This method simplifies the network by assigning each gene as an independent node connected to others by the pairwise correlation. The size of the communities is defined by the value of k and the minimum correlation that connects nodes is defined by the threshold, I. A value of $k = 4$ was chosen to balance the number of internally connected communities and the cohesion of the community[32,48,49] and the optimized I was identified to be 0.68 (Figure S6). There were three large communities and one small community identified under these conditions (Figure 4B). Gene ontology (GO) enrichment analysis was employed to identify and assess overrepresented biological processes unique to each network community. Of interest are processes related to cell health and fitness during stress, which are closely related to cell cycle/differentiation/apoptosis, metabolism, transcriptional/translational control, and response to internal and external changes.[24,50,51] Enriched across the entire heritable gene pool were 11 children GO terms relating to the response to stimuli, including the response to chemical, external stimuli, and stress. Likewise, 5 children terms relating to apoptotic processes were enriched, most notably the regulation of apoptosis. These two biological processes constitute the immediate detection of external stress and the resulting response for unresolved stress when cytoprotective forces are insufficient to promote cell survival.[52] Other noteworthy clusters include regulation of cell adhesion, cell communication, and cellular compartmentalization (Figure 4C). In addition to genes relating to these two biological processes and specific to certain community networks identifier, there were other noteworthy enriched terms including cell cycle/proliferation, regulation of gene expression due to epigenetics/protein activity, and cell differentiation (Figure S7). These networks may outline orthogonal mechanisms for how CHO develops a stress-tolerant phenotype. The rare and random fluctuation of a stress-tolerance gene that displays heritable characteristics into a high expression state would poise a small population of cells to be ready to combat the deleterious effects of the stressors while conferring favorable growth kinetics or survivability that are inherited by the progeny. In this specific context, the mechanism behind the co-fluctuations is not well understood, but may be mutually linked to the expression or activation of common upstream regulatory factors, related to the spatial proximity of the genes as measured through Hi-C sequencing methods, or involve gene regulatory networks.[53–55] For example, *Atf3* negatively co-fluctuates with a subset of genes, indicating their inheritance is directly linked to the inhibition activity of *Atf3*. Provided the co-fluctuation can be replicated, then the transition of any one of the genes within the network community may cascade until a comprehensive stress-tolerant phenotype develops. In this sense, even though individually the rare phenotype may only be present at low frequencies, there are multiple pathways for achieving a similarly tolerant phenotype and increases the likelihood that cells may rapidly adapt.

Combination of MemorySeq fluctuation analysis and differential gene expression analysis highlights promising biomarkers for cell-line engineering

While the MemorySeq data are enriched in stress-tolerance phenotypes, it does not specify which genes correspond to which stressors. To explore this relationship, CHOZN GS$^{-/-}$ Clone 23 was grown in production fed-batch flasks in the presence of biomanufacturing-relevant levels of ammonia, lactate, and osmolality provided these chemicals hinder cell growth kinetics and reduces overall cell health[22,28,56] (Figure S8). These stressors were chosen as they could be chemically manipulated in a fed-batch shake flask environment unlike shear stress or gas sparging. Ammonia and lactate accumulate as a waste product from an inefficient overflow metabolism, primarily from glutamine metabolism and glycolysis. Osmolality primarily accumulates during pH maintenance. Under fed-batch conditions, ammonia, lactate, and salt concentrations reach as high as 10–20 mM, 15 mM, and 450 mOsm/kg.[22,27,29,57] Consistent with literature, high levels of ammonia and osmolality resulted in a reduction in IVCD, while lactate appeared to be less impactful (Figure S8). The specific productivity was significantly reduced during ammonia stress and increased during osmotic stress, likely a result of cell swelling. Other notable conditions include shear, oxidative stress, toxic TCA intermediates, and pH and during perfusion operation this may include high-cell densities and shear from tangential flow filtration.[58]

The intersection between DEG and genes identified as heritable may suggest a possible route for which the stress-tolerance phenotype developed. Day 5 fed-batch RNA samples were collected from the high ammonia, lactate, osmolality, and combination of the three for differential gene expression analysis (DGEA). While all samples displayed a shift in gene expression, in agreement with the growth, productivity, and viability data, there was a muted difference between high lactate and the control (Figure S9). The combinatorial stress condition had the most DEGs at 1275 and high lactate had the least at 155 DEGs. For each stress condition, the ratio of DEGs that were heritable to total DEGs significantly exceeded the expected ratio (Chi-squared goodness of fit test, $p < 0.001$) given 10,106 genes from DGEA met filter parameters and 199 of these genes were considered heritable (Table 1). This finding reinforces our hypothesis that the heritable gene expression states significantly overlap with stress responsive genes. GO enrichment analysis was conducted on the overlapping DEG and heritable genes for each stress condition. Between all four conditions, biological processes related to response to stimuli, metabolism, and regulation of apoptosis/cell-cycle were over-represented. These biological processes outline the recognition of an environmental stress, shift in intracellular conditions, and the phenotypic outcome of cell health (Figure S9).

Genes with biological processes related to stress response and cell-health were extracted for all heritable genes. Inspection of these vital biological processes revealed that 30%–50% of heritable genes related to the downregulation of apoptosis were significantly overexpressed in the stressed cultures except

Table 1. Relative enrichment of genes with heritable expression states within the DEG pool

Stress condition	Observed *DEG and Heritable* / *DEG*	Expected *DEG and Heritable* / *DEG*
Ammonia	61 / 704	14 / 704
Lactate	17 / 155	3 / 155
Osmolality	77 / 1147	23 / 1147
Combination	96 / 1275	25 / 1275

Provided there were 199 heritable gene states out of the 10,106 genes considered, the expected ratio would be roughly 2%. Significant difference observed between the observed ratio and expected (Chi-Squared Goodness of Fit Test, $p < 0.001$).

for lactate. Provided that these cells represent stress-shocked cells and not stress-adapted cells, the shifts in gene expression are somewhat obfuscated as there is not an immediate means by which to differentiate what is the stress signal or stress response. Some intuition on their biological function may motivate whether increased expression is associated with stress tolerance, such as with *Hmox1* and *Nnmt* which have been directly shown to display cytoprotective properties in response to oxidative and other sources of stress. However, for other genes, such as *Atf3*, *Tp63*, and *Ier3*, where they may play a role in both anti- and pro-apoptotic pathways depending on the cell-type and stress identity, further engineering or characterization is required. However, their transgenerational properties and association with a stress phenotype warrants further investigation and may constitute a cell line engineering target that may either overexpressed if associated with stress response or repressed if associated with the stress signal. Of the four heritable genes related to the endoplasmic reticulum unfolded protein response (ER UPR), *Atf3*, *Ccnd1*, and *Ddit3* were downregulated across the four stress conditions (Figure 5).[59,60] Each of these genes play a role in the UPR and other stress response pathways to combat ER or external stress signals through induction of apoptosis.[61–64] Their involvement in ER stress and regulation of apoptosis suggests another mechanism for how resistance develops in biopharmaceutical producing CHO cells where external stress compounds upon the metabolic burden of mAb production. The specifics of their regulation are similarly confounded in the stress response or stress signal perspective where overexpression of *Ccnd1* is anti-apoptotic, *Ddit3* is prop-apoptotic, and *Atf3* is context-dependent. For many of these genes, this is the first work to identify them for stress and cell-health association. For others, there is a large body of work that has investigated gene function and role in apoptosis or cell-health, but outside of *Ccnd1*, not often in CHO.[65] In cell lines such as HEK293T and HeLa, the knockout of *Hmox1* contributed to DNA replication stress and worsened culture duration while *Ier3* knockout prevented TAp73β-facilitated apoptosis.[66,67]

The lifetime of these heritable expression states was estimated to be between 5 and 10 generations for all genes identified here (See File S3) assuming a 1% frequency of the rare phenotype in bulk populations as affirmed in the original MemorySeq work, smRNA-FISH, and flow cytometry.[32] The lifetime, which monotonically increases with measured coefficient of variation, provides some insight on gene states that may have more robust mechanisms for maintaining rare phenotypes and are perhaps more key to the early emergence of resistance pathways. While it may not be the case that a rare phenotype with a frequency of 1% is capable of fully penetrating the population during bioreactor operation, stress tolerance can be approached from different starting points as suggested by the co-fluctation network data. This nuance was pointed out in previous work using *EGFR* as a biomarker for resistance to the drug *vemurafenib*,[68] where only about 20% of the upregulated genes from *EGFR*-high cells were also upregulated in drug-resistant cells. This indicated that one biomarker is not sufficient to characterize a stress-resistant phenotype and that pre-resistant and

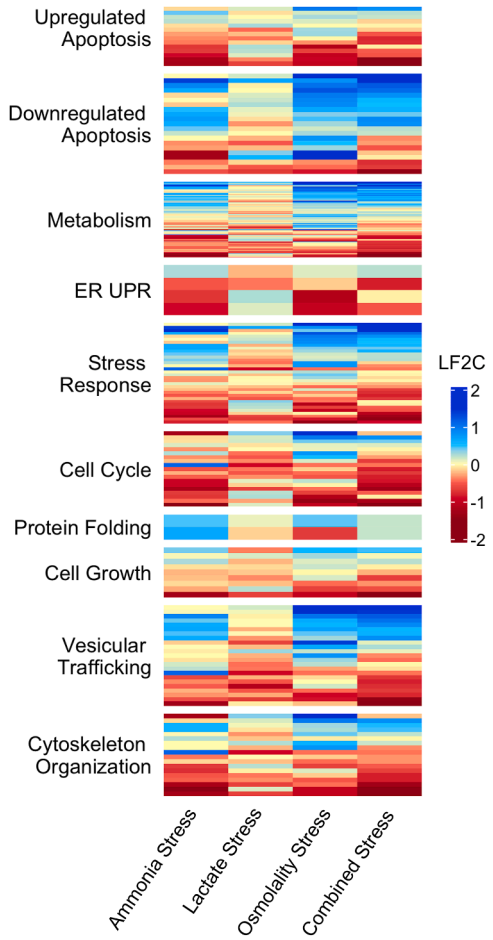

Figure 5. Combination of MemorySeq fluctuation analysis and differential gene expression analysis highlights promising biomarkers for cell-line engineering

Relative gene expression of genes with heritable expression states for common stress response pathways. Heatmap of log fold$_2$ change (LF2C) of heritable gene expression states compared to control fed-batch flask for high ammonia, lactate, osmolality, and combination.

Table 2. Overview of promising biomarkers that exhibit heritable properties and play a role in stress adaptation or response

Gene symbol	Stress condition	Log_2(FC)	Generation lifetime of ON state	Relevant biological processes	References
Hmox1	Ammonia	1.38	5.50	Provides cytoprotective forces against cellular and oxidative stress. Active in cell proliferation and anti-apoptotic processes	Zhu et al.[118]; Funes et al.[119]; Orellana et al.[120]
	Lactate	0.68			
	Osmolality	0.83			
	Everything	1.64			
Serpine1	Ammonia	0.63	5.53	Anti-apoptotic processes and enhanced proliferation upon activation of Akt and ERK signaling pathway. Also shown to correlate with higher productivity in CHO.	Pavón et al.[121]; Zhang et al.[122]; Pavón et al.[123]; Zhou et al.[124]; Ma and Chung[125]
	Lactate	−0.33**			
	Osmolality	0.29**			
	Everything	0.84			
Ier3	Ammonia	0.03*	5.48	Early response gene that responds to environmental stimuli and is regulated by ERK signaling pathway. Regulates apoptosis in a cell-dependent manner	Jin et al.[67]; Shahid et al.[126]; Zhou et al.[127]; Arlt and Schäfer[128]
	Lactate	0.15*			
	Osmolality	2.17			
	Everything	1.78			
Nnmt	Ammonia	−1.15	4.96	Reduce apoptosis through the mitochondria-mediated pathway. Silencing inhibits cell proliferation. Provides resistance to oxidative stress	Zhang et al.[129]; Xie et al.[130]
	Lactate	0.19**			
	Osmolality	−0.17**			
	Everything	−0.80			
Tp63	Ammonia	−1.33	5.95	Acts as a sequence specific DNA binding transcriptional activator or repressor. May be required in conjunction with TP73/p73 for initiation of p53/TP53 dependent apoptosis. Cell-line dependent behavior	Somerville et al.[131]; Melino[132]
	Lactate	−0.24*			
	Osmolality	−0.66			
	Everything	−2.07			
Hmgcs2	Ammonia	0.01*	6.35	Catalyzes step in ketogenesis, condensing acetyl-CoA to acetoacetyl-CoA to form HMG-CoA. Plays a role in cholesterol biosynthetic pathway and expands secretory framework	Chen et al.[133]; Chevallier et al.[134]
	Lactate	−0.70			
	Osmolality	0.64			
	Everything	−0.92			
ATF3	Ammonia	−0.90	5.03	Functions as an oncogene in prostate cancer by enhancing cell proliferation, gene regulation by recruiting p300, and stress response. Appears to co-localize with p53	Edagawa et al.[60]; Zhao et al.[61]; Ku and Cheng[135]
	Lactate	0.13*			
	Osmolality	−0.99			
	Everything	−0.54**			

Summarizes LF2C for different stress conditions and the relevant biological function.
*$p > 0.05$ and $|L2FC|<0.58$.
**$p < 0.05$ and $|L2FC|<0.58$.

resistant phenotypes are biologically distinct. From this analysis, 7 promising biomarkers for resistance to manufacturing stressors were identified (Table 2). This list includes genes that were upregulated across many of the stress conditions, were identified as heritable, and have been previously characterized as influencing apoptotic processes.

DISCUSSION

Biopharmaceutical manufacturing stress is an often-unavoidable obstacle for CLD and production at large-scale and can significantly alter cell line performance with regards to cell health, productivity, and product quality. There is a large body of research investigating apoptotic and proliferation related genes in CHO with the intended purpose of prolonging culture duration and engineering robust cells for therapeutic production. These efforts have identified overexpression of *Bcl-2* and *c-Myc* or knockdown of *Bak*, *Bax*, *Bad*, and *Caspase3/8/9* yield improved growth.[69–72] This work sought to expand the list of possible targets for cell line engineering by outlining a comprehensive and robust workflow for interpreting transcriptomics information to identify stress-dependent biomarkers that improve cell performance during production. Many of these genes do not feature annotations directly related to cell health or their effects are ambiguous and are often ignored during conventional transcriptomic analyses. Analysis tools such as bulk RNA-seq and scRNAseq have been utilized to characterize population-based gene expression and monitor, to a lesser extent, cell-to-cell heterogeneity, but they fail to capture the generational variability and the development of novel phenotypic patterns.[73,74] Bulk RNA-seq is well-suited for measuring broad changes in gene expression, but due to an intrinsic sampling bias when collecting

from a large population, it can under or over predict rare phenotypes.[74,75] By contrast, scRNAseq samples the transcriptomic profile from individual cells isolated from the bulk population. The single-cell resolution of gene expression provides significant information on cellular heterogeneity but is limited on sample size, is difficult to connect to multi-omic datasets, and cannot track the shared lineage between cells without the use of extensive bar-coding.[76] Efforts to characterize single-cell heterogeneity in CHO have been mired by the intrinsic noise contained within. A pair of scRNAseq experiments considering CHO and HEK293T identified an increase in heterogeneity as a result of increased population doubling levels (PDLs) and storage conditions, but was only able to identify one gene, enolase as the sole biomarker that characterized distinct subpopulations using a similar heuristic of CV scaled to transcriptional level.[77,78] While they were unable to find any marker genes for subpopulations, the GO terms of the highly variable genes they did collect shared similar themes as the ones found in this work for heritable genes. This includes response to stimuli, cell-cycle regulation, and cell differentiation.[78] By expanding cells in parallel, as described in the MemorySeq workflow, each of the monoclonal-derived cell pools have a shared internal lineage. The heterogeneity in gene expression that is measured is therefore a reflection of intermediate transcriptional fluctuations that are time dependent as well as natural genetic drift. If the monoclonal expansion were carried out well beyond 100,000 clones, the RNA-seq profile would gradually shift toward the bulk RNA-seq result captured from the noise control.

Leveraging MemorySeq tools, this is the first body of work that seeks to identify biomarkers for pre-stress tolerance in CHO using heritability principles. Ammonia stress has been shown to influence glycosylation, amino acid metabolism, and induce genomic instability in the form of indels and SNPs. Using bulk RNA-seq to measure transcriptional shifts for ammonia-stressed CHO cells, genes relating to alanine metabolism, cell-cycle regulation, cellular senescence, and DNA damage/repair were identified as possibly contributing to impaired growth and productivity kinetics.[22,27] However, there was no metric for discerning the noise of DEGs and those that could play a key role in stress adaption. MemorySeq highlights gene states that play a crucial role in the transition to a stress tolerant state. However, not all genes may necessarily be responsible for the tolerance phenotype.[68] By combining MemorySeq with stress adapted DEG, this method narrows the list down to possible entry points into stress response pathways. Similarly, exploratory works in hyperosmolar stress conditions characterized the same effect of enhanced specific productivity and reduced growth rate. Transcriptomic and proteomic analysis identified mitochondrial activation, oxidative stress reduction, and cell cycle progression as playing a role in hyperosmolar stress response, but could not comment further as to which genes were most important in the developing stress adapted phenotype.[56,79] Previous literature has widely considered the phenotypic and surface-level proteomic changes associated with manufacturing stress conditions but has not reflected on the possible pathways for stress adaptation.

There are many cell line engineering strategies available for targeting these biomarkers to induce a stress-resistant phenotype. If the activation of a gene is correlated with stress-tolerance, gene overexpression could be achieved by integrating additional copies or using inactivated Cas9 (dCas9)-directed activation (CRISPRa) to enhance stress adaptation.[80–82] This approach has proven effective for the reduction of apoptosis, autophagy, and cell proliferation where incorporating additional copies of genes such as *Bcl-2/Beclin-1*, *Ccnd1*, and *c-Myc* was capable of extending culture duration by two or more days, increased IVCD my more than 20%, and reduced early stage apoptosis by over 35%.[65,70,83] This work is intended to generate unique targets for similar engineering that not only cf. favorable growth, but tolerance to the stress associated with production. Inherently, stress tolerance is an anti-apoptotic or pro-proliferation process, so while overexpression may cf. a slight burden, it is offset by the concomitant improved growth. Likewise, if the repression of a gene is correlated with stress-resistance, gene knockout or knockdown-methods such as RNA interference (RNAi), Cas9-facilitated knockout, or dCas9-directed inhibition (CRISPRi) could also be employed for the same effect.[84,85] However, stress response pathways are composed of many proteins that influence a variety of molecular functions to accommodate and mitigate the deleterious effects of stress. Methods that target a single gene may not always activate a whole pathway but lessen only one symptom of the stress.[86,87] Activation of response pathways develops a more robust stress response to tackle the multi-faceted burden of cellular stress.[88,89] These stress-responsive pathways have been noted in CHO to alleviate oxidative-stress associated with production and bioreactor conditions that involve anti-apoptotic and GSH biosynthetic pathways.[90–92] In this work, 4 co-fluctuating community networks that contain genes relating to stress detection and critical cell health processes were identified and may demonstrate critical entry points into stress response pathways. Similar to the involvement of *Bcl-2* in the signaling pathway for other cell health markers, such as the *PI3K/Akt* survival pathway or caspase proteins, genes within these communities may serve similar signaling or regulatory roles to cf. favorable and robust cell health.[93,94]

It is believed that these heritable, but ultimately transient fluctuations in expression are largely due to epigenetic modifications and gene regulatory networks within the co-fluctuating communities. While no comparable study has been conducted in CHO, temperature, nutrient, and osmolality induced environmental stress has resulted in epigenetically driven and inherited stress tolerant states in other organisms. In *S. cerevisiae* during periods of inositol starvation and osmotic stress, accumulation of di- and tri-methylation of H3K4 histone marks was observed following a period of hyperacetylation of H3 and H4.[95,96] This state correlated to the recruitment of the SET3C complex that reinforced an active heritable memory state that facilitated the recruitment of poised RNAPII lasting 4–8 generations.[96] A similar pattern of H3K4me2 deposition and transgenerational inheritance of stress resistance has been observed in eukaryotic organisms such as HeLa and *D. melanogaster* cells as facilitated by the nuclear pore protein Nup98.[97–99] Definitive identification of the source of heritable expression states would require capturing a single cell displaying the rare phenotype and characterizing the epigenetic and transcriptomic state using single-cell methods, such

as scRNAseq, scATACseq, and scChIPseq. The chromatin structure of the DNA is complex and forms conserved connections across chromosomes and between genes that are otherwise not proximal or contiguous in the linear genome[55,100] Co-regulation may become a function of local chromatin structures and the cross-talk of epigenetic marks and may outline another engineering approach utilizing site-specific epigenetic modifications to simulate the natural transition to rare phenotypes.

While the mechanism for the intermediate heritable states described in this worked are still ambiguous, these states also appear to be a combination of conserved and cell line specific processes. When compared to the original MemorySeq work performed in WM989 and WM983B melanoma, MDA breast cancer, and PC9 carcinoma cell lines, anywhere from 4% to 10% of the heritable gene states unique to these cell lines appeared in our CHO cell line. Across all four of the cell lines, 16.5% of the genes there were identified as heritable in this work appeared heritable in at least one of the other cell lines, including *Hmox1*, *Ier3*, and *Serpine1*.[32] These shared gene states may represent some form of evolutionarily conserved states that serve as important entry points to the transition to stress tolerance.

Ultimately, this study sought to expand our understanding of CHO cell stress adaptation. The deleterious phenotypic effects of common manufacturing stressors, such as ammonia, lactate, and osmolality, observed in literature were likewise observed here. However, using the non-conventional transcriptomic workflow described in MemorySeq, the process for parsing the transcriptional noise that the stresses induce becomes more meaningful. The combination of information obtained from stress-induced cultures and MemorySeq reinforces our understanding of manufacturing stress while highlighting diagnostic genes for the rational design of engineered cell lines. While the exact mechanism of the two-state systems observed here remains unclear, their observation in other systems reinforces the idea that epigenetics and, to some extent, stochasticity play an important role. Such epigenetically driven, metastable, long-term memory states have been elucidated in epithelial tissue and *S. enterica* to adapt to perturbations within the environment.[13,14] Being able to harness what is otherwise a natural and random adaptation phenomenon into an intentionally engineered pathway will lead to CHO strain that is primed for the strain of manufacturing-scale condition. Healthier cells remain more productive for longer and alleviate the burden of downstream purification. This pipeline for assessing stress-dependent effects is also translatable to other cell lines and other stress conditions, expanding our ability to identify cell line engineering targets and streamline CLD processes.

Limitations of the study

In this work, we outline a robust workflow for identifying stress-associated biomarkers. The intention with this work is to propose a method to interpret noise traditionally observed in RNA-seq data. There are two primary limitations of this work described here. The first of which concerns the claims of epigenetic driven inheritance and the risk regulatory gene networks dominate the observations of heritability. While we do observe conserved repressive epigenetic marks concentrated on these heritable genes, it becomes difficult to deconvolute these two phenomena and are at risk of enriching the heritable gene pool with genes that are mutually regulated by similar transcription factors and not by spontaneous epigenetic deviations. It would be valuable to supplement this study with the full panel of epigenetic characterizing methods alongside RNA-seq to determine if changes in average expression are accompanied by changes in the epigenome.

The second concern relates to the population of DEGs following stress shock during fed-batch. It is unclear from the RNA-seq data whether DEGs reflect a stress signal or stress response pathway. In some cases, the answer may be deciphered by considering biological function. For example, *Hmox1* is a known anti-apoptotic gene and its upregulation would be beneficial to the cell. Other genes are more ambiguous or are not annotated with a related. We believe that regardless of which pathway is involved, the gene itself remains a viable biomarker for cell line engineering. However, it may require investigating both overexpression and repression to identify the mode of action. An additional study measuring differential gene expression in stress-adapted cells, or cells passaged in the presence of stress until cell-specific growth rate is recovered, may resolve this uncertainty.

RESOURCE AVAILABILITY

Lead contact

Requests for further information and resources should be directed to and will be fulfilled by the lead contact, Mark Blenner (blenner@udel.edu).

Materials availability

This study did not generate new unique reagents.

Data and code availability

RNA sequencing data have been deposited at the GEO repository and are publicly available as of the date of publication. Accession numbers are listed in the key resources table. In addition, code for RNA sequencing and MemorySeq processing and analysis have been deposited on GitHub are publicly available as of the date of publication. GitHub links are listed in the key resources table.

All data reported in this paper will be shared by the lead contact upon request. RNA sequencing data have been deposited at the GEO repository and are publicly available as of the date of publication. Accession numbers are listed in the key resources table. In addition, code for RNA sequencing and MemorySeq processing and analysis have been deposited on GitHub are publicly available as of the date of publication. GitHub links are listed in the key resources table. Any additional information required to reanalyze the data reported will be shared by the lead contact upon request. Any additional information required to reanalyze the data reported will be shared by the lead contact upon request.

ACKNOWLEDGMENTS

We thank the Expression Systems and Novel Biopharm Materials Team at MilliporeSigma for access to the CHOZN GS$^{-/-}$ Clone 23 cell line; Dyllan Rives for aiding in cell culture; Molly Wintenberg for providing RNA-seq analysis pipeline for CHO, Sylvain Le Marchand with the Delaware Biotechnology Institute's Bio-Imaging Center for instruction and experimental planning for smRNA-FISH; Erin Bernberg and Mark Shaw with the Delaware Biotechnology Institute's Sequencing and Genotyping for aid in RNA extractions and quality verification; Ross Klauer, Emily Doleh, Christopher Pirner for reviewing and editing the paper. This work was supported by funding from the UD College of Engineering. A.S. acknowledges the support of NIH-NIGMS via grant R35GM148351.

AUTHOR CONTRIBUTIONS

Conceptualization, S.G., A.S., and M.B.; methodology, S.G., A.S., and M.B.; software, S.G. and Z.D.; formal analysis S.G., A.S., and Z.D.; investigation, S.G. and Z.D.; visualization, S.G. and Z.D.; data curation, S.G.; writing – original draft, S.G.; writing – review and editing, S.G., A.S., and M.B.; resources, M.B., supervision, M.B.; funding acquisition, M.B.

DECLARATION OF INTERESTS

The authors declare no competing interests.

STAR★METHODS

Detailed methods are provided in the online version of this paper and include the following:

- KEY RESOURCES TABLE
- EXPERIMENTAL MODEL AND STUDY PARTICIPANT DETAILS
  - Cell lines and culture maintenance
- METHOD DETAILS
  - Single cell limited dilution cloning
  - RNA extraction and sequencing
  - smRNA-FISH and imaging
  - Stress-condition fed-batch
- QUANTIFICATION AND STATISTICAL ANALYSIS
  - MemorySeq processing
  - Prediction of heritability lifetime index
  - Epigenome characterization relative to published data
  - Stress-condition fed-batch analysis

SUPPLEMENTAL INFORMATION

Supplemental information can be found online at https://doi.org/10.1016/j.isci.2025.113478.

Received: February 4, 2025
Revised: June 30, 2025
Accepted: August 28, 2025
Published: September 1, 2025

REFERENCES

1. Wildt, S., and Gerngross, T.U. (2005). The humanization of N -glycosylation pathways in yeast. Nat. Rev. Microbiol. *3*, 119–128.
2. Brooks, S.A. (2004). Appropriate glycosylation of recombinant proteins for human use. Mol. Biotechnol. *28*, 241–255.
3. Lee, J.S., Kildegaard, H.F., Lewis, N.E., and Lee, G.M. (2019). Mitigating clonal variation in recombinant mammalian cell lines. Trends Biotechnol. *37*, 931–942.
4. Kim, M., O'Callaghan, P.M., Droms, K.A., and James, D.C. (2011). A mechanistic understanding of production instability in CHO cell lines expressing recombinant monoclonal antibodies. Biotechnol. Bioeng. *108*, 2434–2446.
5. Keung, A.J., Joung, J.K., Khalil, A.S., and Collins, J.J. (2015). Chromatin regulation at the frontier of synthetic biology. Nat. Rev. Genet. *16*, 159–171.
6. Park, M., Keung, A.J., and Khalil, A.S. (2016). The epigenome: the next substrate for engineering. Genome Biol. *17*, 183.
7. Turner, B.M. (2009). Epigenetic responses to environmental change and their evolutionary implications. Philos. Trans. R. Soc. Lond. B Biol. Sci. *364*, 3403–3418.
8. Feichtinger, J., Hernández, I., Fischer, C., Hanscho, M., Auer, N., Hackl, M., Jadhav, V., Baumann, M., Krempl, P.M., Schmidl, C., et al. (2016). Comprehensive genome and epigenome characterization of CHO cells in response to evolutionary pressures and over time. Biotechnol. Bioeng. *113*, 2241–2253.
9. Veith, N., Ziehr, H., MacLeod, R.A.F., and Reamon-Buettner, S.M. (2016). Mechanisms underlying epigenetic and transcriptional heterogeneity in Chinese hamster ovary (CHO) cell lines. BMC Biotechnol. *16*, 6.
10. Hernandez, I., Dhiman, H., Klanert, G., Jadhav, V., Auer, N., Hanscho, M., Baumann, M., Esteve-Codina, A., Dabad, M., Gómez, J., et al. (2019). Epigenetic regulation of gene expression in Chinese Hamster Ovary cells in response to the changing environment of a batch culture. Biotechnol. Bioeng. *116*, 677–692.
11. Bintu, L., Yong, J., Antebi, Y.E., McCue, K., Kazuki, Y., Uno, N., Oshimura, M., and Elowitz, M.B. (2016). Dynamics of epigenetic regulation at the single-cell level. Science *351*, 720–724.
12. Lensch, S., Herschl, M.H., Ludwig, C.H., Sinha, J., Hinks, M.M., Mukund, A., Fujimori, T., and Bintu, L. (2022). Dynamic spreading of chromatin-mediated gene silencing and reactivation between neighboring genes in single cells. eLife *11*, e75115.
13. Fernández-Fernández, R., Olivenza, D.R., Weyer, E., Singh, A., Casadesús, J., and Sánchez-Romero, M.A. (2024). Evolution of a bistable genetic system in fluctuating and nonfluctuating environments. Proc. Natl. Acad. Sci. USA *121*, e2322371121.
14. Clark, H.R., McKenney, C., Livingston, N.M., Gershman, A., Sajjan, S., Chan, I.S., Ewald, A.J., Timp, W., Wu, B., Singh, A., and Regot, S. (2021). Epigenetically regulated digital signaling defines epithelial innate immunity at the tissue level. Nat. Commun. *12*, 1836.
15. Schuh, L., Saint-Antoine, M., Sanford, E.M., Emert, B.L., Singh, A., Marr, C., Raj, A., and Goyal, Y. (2020). Gene networks with transcriptional bursting recapitulate rare transient coordinated high expression states in cancer. Cell Syst. *10*, 363–378.e12.
16. Gómez-Schiavon, M., and Buchler, N.E. (2019). Epigenetic switching as a strategy for quick adaptation while attenuating biochemical noise. PLoS Comput. Biol. *15*, e1007364.
17. Park, J., Lim, C.J., Shen, M., Park, H.J., Cha, J.Y., Iniesto, E., Rubio, V., Mengiste, T., Zhu, J.K., Bressan, R.A., et al. (2018). Epigenetic switch from repressive to permissive chromatin in response to cold stress. Proc. Natl. Acad. Sci. USA *115*, E5400–E5409.
18. Walter, M., Teissandier, A., Pérez-Palacios, R., and Bourc'his, D. (2016). An epigenetic switch ensures transposon repression upon dynamic loss of DNA methylation in embryonic stem cells. eLife *5*, e11418.
19. Ravindran Menon, D., Hammerlindl, H., Torrano, J., Schaider, H., and Fujita, M. (2020). Epigenetics and metabolism at the crossroads of stress-induced plasticity, stemness and therapeutic resistance in cancer. Theranostics *10*, 6261–6277.
20. Sharma, S.V., Lee, D.Y., Li, B., Quinlan, M.P., Takahashi, F., Maheswaran, S., McDermott, U., Azizian, N., Zou, L., Fischbach, M.A., et al. (2010). A chromatin-mediated reversible drug-tolerant state in cancer cell subpopulations. Cell *141*, 69–80.
21. Henrique, R., Oliveira, A.I., Costa, V.L., Baptista, T., Martins, A.T., Morais, A., Oliveira, J., and Jerónimo, C. (2013). Epigenetic regulation of MDR1 gene through post-translational histone modifications in prostate cancer. BMC Genom. *14*, 898.
22. Chitwood, D.G., Wang, Q., Elliott, K., Bullock, A., Jordana, D., Li, Z., Wu, C., Harcum, S.W., and Saski, C.A. (2021). Characterization of metabolic responses, genetic variations, and microsatellite instability in ammonia-stressed CHO cells grown in fed-batch cultures. BMC Biotechnol. *21*, 4.
23. Schellenberg, J., Nagraik, T., Wohlenberg, O.J., Ruhl, S., Bahnemann, J., Scheper, T., and Solle, D. (2022). Stress-induced increase of monoclonal antibody production in CHO cells. Eng. Life Sci. *22*, 427–436.
24. Shen, D., Kiehl, T.R., Khattak, S.F., Li, Z.J., He, A., Kayne, P.S., Patel, V., Neuhaus, I.M., and Sharfstein, S.T. (2010). Transcriptomic responses to sodium chloride-induced osmotic stress: A study of industrial fed-batch CHO cell cultures. Biotechnol. Prog. *26*, 1104–1115.

25. Sieck, J.B., Villiger, T., Budach, W.E., Suemeghy, Z., Leist, C., Morbidelli, M., and Soos, M. (2012). Response of a CHO production cell line to different types of hydrodynamic shear stress present in stirred and sparged bioreactors. N. Biotechnol. *29*, S165.

26. Handlogten, M.W., Zhu, M., and Ahuja, S. (2018). Intracellular response of CHO cells to oxidative stress and its influence on metabolism and antibody production. Biochem. Eng. J. *133*, 12–20.

27. Synoground, B.F., McGraw, C.E., Elliott, K.S., Leuze, C., Roth, J.R., Harcum, S.W., and Sandoval, N.R. (2021). Transient ammonia stress on Chinese hamster ovary (CHO) cells yield alterations to alanine metabolism and IgG glycosylation profiles. Biotechnol. J. *16*, 2100098.

28. Li, J., Wong, C.L., Vijayasankaran, N., Hudson, T., and Amanullah, A. (2012). Feeding lactate for CHO cell culture processes: Impact on culture metabolism and performance. Biotechnol. Bioeng. *109*, 1173–1186.

29. Slivac, I., Blajić, V., Radošević, K., Kniewald, Z., and Gaurina Srček, V. (2010). Influence of different ammonium, lactate and glutamine concentrations on CCO cell growth. Cytotechnology *62*, 585–594.

30. Tauffenberger, A., Fiumelli, H., Almustafa, S., and Magistretti, P.J. (2019). Lactate and pyruvate promote oxidative stress resistance through hormetic ROS signaling. Cell Death Dis. *10*, 653.

31. Zagari, F., Jordan, M., Stettler, M., Broly, H., and Wurm, F.M. (2013). Lactate metabolism shift in CHO cell culture: the role of mitochondrial oxidative activity. N. Biotechnol. *30*, 238–245.

32. Shaffer, S.M., Emert, B.L., Reyes Hueros, R.A., Cote, C., Harmange, G., Schaff, D.L., Sizemore, A.E., Gupte, R., Torre, E., Singh, A., et al. (2020). Memory sequencing reveals heritable single-cell gene expression programs associated with distinct cellular behaviors. Cell *182*, 947–959.e17.

33. Luria, S.E., and Delbrück, M. (1943). Mutations of bacteria from virus sensitivity to virus resistance. Genetics *28*, 491–511.

34. Guha, M., Singh, A., and Butzin, N.C. (2025). Priestia megaterium cells are primed for surviving lethal doses of antibiotics and chemical stress. Commun. Biol. *8*, 206.

35. Petkidis, A., Suomalainen, M., Andriasyan, V., Singh, A., and Greber, U.F. (2024). Preexisting cell state rather than stochastic noise confers high or low infection susceptibility of human lung epithelial cells to adenovirus. mSphere *9*, e0045424.

36. Dhama, K., Latheef, S.K., Dadar, M., Samad, H.A., Munjal, A., Khandia, R., Karthik, K., Tiwari, R., Yatoo, M.I., Bhatt, P., et al. (2019). Biomarkers in stress related diseases/disorders: Diagnostic, prognostic, and therapeutic values. Front. Mol. Biosci. *6*, 91.

37. Wang, L., Feng, Z., Wang, X., Wang, X., and Zhang, X. (2010). DEGseq: an R package for identifying differentially expressed genes from RNA-seq data. Bioinformatics *26*, 136–138.

38. Auer, P.L., and Doerge, R.W. (2011). A two-stage poisson model for testing RNA-seq data. Stat. Appl. Genet. Mol. Biol. *10*.

39. Brown, R., Curry, E., Magnani, L., Wilhelm-Benartzi, C.S., and Borley, J. (2014). Poised epigenetic states and acquired drug resistance in cancer. Nat. Rev. Cancer *14*, 747–753.

40. Tomasin, R., and Ghajar, C.M. (2024). Poised epigenetic states dictate metastatic fitness. Trends Cancer *10*, 275–276.

41. Elliott, G., Hong, C., Xing, X., Zhou, X., Li, D., Coarfa, C., Bell, R.J.A., Maire, C.L., Ligon, K.L., Sigaroudinia, M., et al. (2015). Intermediate DNA methylation is a conserved signature of genome regulation. Nat. Commun. *6*, 6363.

42. Sharifi-Zarchi, A., Gerovska, D., Adachi, K., Totonchi, M., Pezeshk, H., Taft, R.J., Schöler, H.R., Chitsaz, H., Sadeghi, M., Baharvand, H., and Araúzo-Bravo, M.J. (2017). DNA methylation regulates discrimination of enhancers from promoters through a H3K4me1-H3K4me3 seesaw mechanism. BMC Genom. *18*, 964.

43. Weber, M., Hellmann, I., Stadler, M.B., Ramos, L., Pääbo, S., Rebhan, M., and Schübeler, D. (2007). Distribution, silencing potential and evolutionary impact of promoter DNA methylation in the human genome. Nat. Genet. *39*, 457–466.

44. Ansel, J., Bottin, H., Rodriguez-Beltran, C., Damon, C., Nagarajan, M., Fehrmann, S., François, J., and Yvert, G. (2008). Cell-to-cell stochastic variation in gene expression is a complex genetic trait. PLoS Genet. *4*, e1000049.

45. Huhn, S., Chang, M., Kumar, A., Liu, R., Jiang, B., Betenbaugh, M., Lin, H., Nyberg, G., and Du, Z. (2022). Chromosomal instability drives convergent and divergent evolution toward advantageous inherited traits in mammalian CHO bioproduction lineages. iScience *25*, 104074.

46. Giusti, C., Pastalkova, E., Curto, C., and Itskov, V. (2015). Clique topology reveals intrinsic geometric structure in neural correlations. Proc. Natl. Acad. Sci. USA *112*, 13455–13460.

47. Rieck, B., Fugacci, U., Lukasczyk, J., and Leitte, H. (2018). Clique community persistence: a topological visual analysis approach for complex networks. IEEE Trans. Vis. Comput. Graph. *24*, 822–831.

48. Palla, G., Derényi, I., Farkas, I., and Vicsek, T. (2005). Uncovering the overlapping community structure of complex networks in nature and society. Nature *435*, 814–818.

49. Jonsson, P.F., Cavanna, T., Zicha, D., and Bates, P.A. (2006). Cluster analysis of networks generated through homology: automatic identification of important protein communities involved in cancer metastasis. BMC Bioinf. *7*, 2.

50. Sha, S., Bhatia, H., and Yoon, S. (2018). An RNA-seq based transcriptomic investigation into the productivity and growth variants with Chinese hamster ovary cells. J. Biotechnol. *271*, 37–46.

51. Fischer, S., Handrick, R., and Otte, K. (2015). The art of CHO cell engineering: A comprehensive retrospect and future perspectives. Biotechnol. Adv. *33*, 1878–1896.

52. Fulda, S., Gorman, A.M., Hori, O., and Samali, A. (2010). Cellular stress responses: Cell survival and cell death. Int. J. Cell Biol. *2010*, 214074.

53. Nie, Z., Hu, G., Wei, G., Cui, K., Yamane, A., Resch, W., Wang, R., Green, D.R., Tessarollo, L., Casellas, R., et al. (2012). c-Myc is a universal amplifier of expressed genes in lymphocytes and embryonic stem cells. Cell *151*, 68–79.

54. Sun, M., and Zhang, J. (2019). Chromosome-wide co-fluctuation of stochastic gene expression in mammalian cells. PLoS Genet. *15*, e1008389.

55. Hilliard, W., and Lee, K.H. (2021). Systematic identification of safe harbor regions in the CHO genome through a comprehensive epigenome analysis. Biotechnol. Bioeng. *118*, 659–675.

56. Alhuthali, S., Kotidis, P., and Kontoravdi, C. (2021). Osmolality effects on CHO cell growth, cell volume, antibody productivity and glycosylation. Int. J. Mol. Sci. *22*, 3290.

57. Schneider, M., Marison, I.W., and von Stockar, U. (1996). The importance of ammonia in mammalian cell culture. J. Biotechnol. *46*, 161–185.

58. Clincke, M.-F., Mölleryd, C., Zhang, Y., Lindskog, E., Walsh, K., and Chotteau, V. (2013). Very high density of CHO cells in perfusion by ATF or TFF in WAVE Bioreactor™. Part I. Effect of the cell density on the process. Biotechnol. Prog. *29*, 754–767.

59. Jiang, Y., Zhang, C., Lu, L., Wang, X., Liu, H., Jiang, Y., Hong, L., Chen, Y., Huang, H., and Guo, D. (2022). The prognostic role of cyclin D1 in multiple myeloma: A systematic review and meta-analysis. Technol. Cancer Res. Treat. *21*, 15330338211065252.

60. Edagawa, M., Kawauchi, J., Hirata, M., Goshima, H., Inoue, M., Okamoto, T., Murakami, A., Maehara, Y., and Kitajima, S. (2014). Role of activating transcription factor 3 (ATF3) in endoplasmic reticulum (ER) stress-induced sensitization of p53-deficient human colon cancer cells to tumor necrosis factor (TNF)-related apoptosis-inducing ligand (TRAIL)-mediated Apoptosis through Up-regulation of Death Receptor 5 (DR5) by Zerumbone and Celecoxib. J. Biol. Chem. *289*, 21544–21561.

61. Zhao, J., Li, X., Guo, M., Yu, J., and Yan, C. (2016). The common stress responsive transcription factor ATF3 binds genomic sites enriched with p300 and H3K27ac for transcriptional regulation. BMC Genom. *17*, 335.

62. Hetz, C. (2012). The unfolded protein response: controlling cell fate decisions under ER stress and beyond. Nat. Rev. Mol. Cell Biol. *13*, 89–102.

63. Jiang, H., Ding, D., He, Y., Li, X., Xu, Y., and Liu, X. (2021). Xbp1s-Ddit3 promotes MCT-induced pulmonary hypertension. Clin. Sci. *135*, 2467–2481.

64. Bustany, S., Cahu, J., Guardiola, P., and Sola, B. (2015). Cyclin D1 sensitizes myeloma cells to endoplasmic reticulum stress-mediated apoptosis by activating the unfolded protein response pathway. BMC Cancer *15*, 262.

65. Zhao, X., Guo, J., Yu, Y., Yi, S., Yu, T., Fu, L., Hou, L., and Chen, W. (2011). Overexpression of survivin and cyclin D1 in CHO cells confers apoptosis resistance and enhances growth in serum-free suspension culture. Biotechnol. Lett. *33*, 1293–1300.

66. Chudy, P., Kochan, J., Wawro, M., Nguyen, P., Gorczyca, M., Varanko, A., Retka, A., Ghadei, S.S., Napieralska, E., Grochot-Przęczek, A., et al. (2024). Heme oxygenase-1 protects cells from replication stress. Redox Biol. *75*, 103247.

67. Jin, H., Suh, D.S., Kim, T.H., Yeom, J.H., Lee, K., and Bae, J. (2015). IER3 is a crucial mediator of TAp73β-induced apoptosis in cervical cancer and confers etoposide sensitivity. Sci. Rep. *5*, 8367.

68. Shaffer, S.M., Dunagin, M.C., Torborg, S.R., Torre, E.A., Emert, B., Krepler, C., Beqiri, M., Sproesser, K., Brafford, P.A., Xiao, M., et al. (2017). Rare cell variability and drug-induced reprogramming as a mode of cancer drug resistance. Nature *546*, 431–435.

69. Latorre, Y., Torres, M., Vergara, M., Berrios, J., Sampayo, M.M., Gödecke, N., Wirth, D., Hauser, H., Dickson, A.J., and Altamirano, C. (2023). Engineering of Chinese hamster ovary cells for co-overexpressing MYC and XBP1s increased cell proliferation and recombinant EPO production. Sci. Rep. *13*, 1482.

70. Lee, J.S., Ha, T.K., Park, J.H., and Lee, G.M. (2013). Anti-cell death engineering of CHO cells: Co-overexpression of Bcl-2 for apoptosis inhibition, Beclin-1 for autophagy induction. Biotechnol. Bioeng. *110*, 2195–2207.

71. Tang, D., Lam, C., Bauer, N., Auslaender, S., Snedecor, B., Laird, M.W., and Misaghi, S. (2022). Bax and Bak knockout apoptosis-resistant Chinese hamster ovary cell lines significantly improve culture viability and titer in intensified fed-batch culture process. Biotechnol. Prog. *38*, e3228.

72. Safari, F., and Akbari, B. (2022). Knockout of caspase-7 gene improves the expression of recombinant protein in CHO cell line through the cell cycle arrest in G2/M phase. Biol. Res. *55*, 2.

73. Varabyou, A., Salzberg, S.L., and Pertea, M. (2021). Effects of transcriptional noise on estimates of gene and transcript expression in RNA sequencing experiments. Genome Res. *31*, 301–308.

74. Li, X., and Wang, C.-Y. (2021). From bulk, single-cell to spatial RNA sequencing. Int. J. Oral Sci. *13*, 36.

75. Gyanchandani, R., Lin, Y., Lin, H.M., Cooper, K., Normolle, D.P., Brufsky, A., Fastuca, M., Crosson, W., Oesterreich, S., Davidson, N.E., et al. (2016). Intratumor heterogeneity affects gene expression profile test prognostic risk stratification in early breast cancer. Clin. Cancer Res. *22*, 5362–5369.

76. Chen, C., Liao, Y., and Peng, G. (2022). Connecting past and present: Single-cell lineage tracing. Protein Cell *13*, 790–807.

77. Ogata, N., Nishimura, A., Matsuda, T., Kubota, M., and Omasa, T. (2021). Single-cell transcriptome analyses reveal heterogeneity in suspension cultures and clonal markers of CHO-K1 cells. Biotechnol. Bioeng. *118*, 944–951.

78. Borsi, G., Motheramgari, K., Dhiman, H., Baumann, M., Sinkala, E., Sauerland, M., Riba, J., and Borth, N. (2023). Single-cell RNA sequencing reveals homogeneous transcriptome patterns and low variance in a suspension CHO-K1 and an adherent HEK293FT cell line in culture conditions. J. Biotechnol. *364*, 13–22.

79. Romanova, N., Schelletter, L., Hoffrogge, R., and Noll, T. (2022). Hyperosmolality in CHO cell culture: effects on the proteome. Appl. Microbiol. Biotechnol. *106*, 2569–2586.

80. Moriya, H. (2015). Quantitative nature of overexpression experiments. Mol. Biol. Cell *26*, 3932–3939.

81. Karottki, K.J.l.C., Hefzi, H., Xiong, K., Shamie, I., Hansen, A.H., Li, S., Pedersen, L.E., Li, S., Lee, J.S., Lee, G.M., et al. (2020). Awakening dormant glycosyltransferases in CHO cells with CRISPRa. Biotechnol. Bioeng. *117*, 593–598.

82. Jiang, Q., Sun, Y., Guo, Z., Fu, M., Wang, Q., Zhu, H., Lei, P., and Shen, G. (2017). Overexpression of GRP78 enhances survival of CHO cells in response to serum deprivation and oxidative stress. Eng. Life Sci. *17*, 107–116.

83. Ifandi, V., and Al-Rubeai, M. (2003). Stable transfection of CHO cells with the c-myc gene results in increased proliferation rates, reduces serum dependency, and induces anchorage independence. Cytotechnology *41*, 1–10.

84. Haiyong, H. (2018). RNA interference to knock down gene expression. Methods Mol. Biol. *1706*, 293–302.

85. Xiong, K., Marquart, K.F., la Cour Karottki, K.J., Li, S., Shamie, I., Lee, J. S., Gerling, S., Yeo, N.C., Chavez, A., Lee, G.M., et al. (2019). Reduced apoptosis in Chinese hamster ovary cells via optimized CRISPR interference. Biotechnol. Bioeng. *116*, 1813–1819.

86. Levine, M.E., and Crimmins, E.M. (2016). A genetic network associated with stress resistance, longevity, and cancer in humans. J. Gerontol. A Biol. Sci. Med. Sci. *71*, 703–712.

87. Soo, S.K., Traa, A., Rudich, Z.D., Moldakozhayev, A., Mistry, M., and Van Raamsdonk, J.M. (2023). Genetic basis of enhanced stress resistance in long-lived mutants highlights key role of innate immunity in determining longevity. Aging Cell *22*, e13740.

88. Kourtis, N., and Tavernarakis, N. (2011). Cellular stress response pathways and ageing: intricate molecular relationships. EMBO J. *30*, 2520–2531.

89. González, C., Ray, J.C.J., Manhart, M., Adams, R.M., Nevozhay, D., Morozov, A.V., and Balázsi, G. (2015). Stress-response balance drives the evolution of a network module and its host genome. Mol. Syst. Biol. *11*, 827.

90. Zustiak, M.P., Jose, L., Xie, Y., Zhu, J., and Betenbaugh, M.J. (2014). Enhanced transient recombinant protein production in CHO cells through the co-transfection of the product gene with Bcl-xL. Biotechnol. J. *9*, 1164–1174.

91. Orellana, C.A., Marcellin, E., Schulz, B.L., Nouwens, A.S., Gray, P.P., and Nielsen, L.K. (2015). High-antibody-producing Chinese hamster ovary cells up-regulate intracellular protein transport and glutathione synthesis. J. Proteome Res. *14*, 609–618.

92. Chevallier, V., Andersen, M.R., and Malphettes, L. (2020). Oxidative stress-alleviating strategies to improve recombinant protein production in CHO cells. Biotechnol. Bioeng. *117*, 1172–1186.

93. Swanton, E., Savory, P., Cosulich, S., Clarke, P., and Woodman, P. (1999). Bcl-2 regulates a caspase-3/caspase-2 apoptotic cascade in cytosolic extracts. Oncogene *18*, 1781–1787.

94. Su, Y., Li, X., Ma, J., Zhao, J., Liu, S., Wang, G., Edwards, H., Taub, J.W., Lin, H., and Ge, Y. (2018). Targeting PI3K, mTOR, ERK, and Bcl-2 signaling network shows superior antileukemic activity against AML *ex vivo*. Biochem. Pharmacol. *148*, 13–26.

95. Fabrizio, P., Garvis, S., and Palladino, F. (2019). Histone methylation and memory of environmental stress. Cells *8*, 339.

96. D'Urso, A., Takahashi, Y.H., Xiong, B., Marone, J., Coukos, R., Randise-Hinchliff, C., Wang, J.P., Shilatifard, A., and Brickner, J.H. (2016). Set1/COMPASS and mediator are repurposed to promote epigenetic transcriptional memory. eLife *5*, e16691.

97. Light, W.H., Freaney, J., Sood, V., Thompson, A., D'Urso, A., Horvath, C. M., and Brickner, J.H. (2013). A conserved role for human Nup98 in altering chromatin structure and promoting epigenetic transcriptional memory. PLoS Biol. *11*, e1001524.

98. Pascual-Garcia, P., Little, S.C., and Capelson, M. (2022). Nup98-dependent transcriptional memory is established independently of transcription. eLife *11*, e63404.

99. Gialitakis, M., Arampatzi, P., Makatounakis, T., and Papamatheakis, J. (2010). Gamma interferon-dependent transcriptional memory via relocalization of a gene locus to PML nuclear bodies. Mol. Cell Biol. *30*, 2046–2056.

100. Zhang, R., Zhou, T., and Ma, J. (2022). Multiscale and integrative single-cell Hi-C analysis with Higashi. Nat. Biotechnol. *40*, 254–261.

101. Rupp, O., MacDonald, M.L., Li, S., Dhiman, H., Polson, S., Griep, S., Heffner, K., Hernandez, I., Brinkrolf, K., Jadhav, V., et al. (2018). A reference genome of the Chinese hamster based on a hybrid assembly strategy. Biotechnol. Bioeng. *115*, 2087–2100.

102. Martin, M. (2011). Cutadapt removes adapter sequences from high-throughput sequencing reads. EMBnet. J. *17*, 10–12.

103. Dobin, A., Davis, C.A., Schlesinger, F., Drenkow, J., Zaleski, C., Jha, S., Batut, P., Chaisson, M., and Gingeras, T.R. (2013). STAR: ultrafast universal RNA-seq aligner. Bioinformatics *29*, 15–21.

104. Li, H., Handsaker, B., Wysoker, A., Fennell, T., Ruan, J., Homer, N., Marth, G., Abecasis, G., and Durbin, R.; 1000 Genome Project Data Processing Subgroup (2009). The sequence alignment/map format and SAMtools. Bioinforma. Oxf. Engl. *25*, 2078–2079.

105. Anders, S., Pyl, P.T., and Huber, W. (2015). HTSeq—a Python framework to work with high-throughput sequencing data. Bioinformatics *31*, 166–169.

106. Feltz, C. J., and Miller, G. E. (1996). An asymptotic test for the equality of coefficients of variation from k populations. Stat. Med. *15*, 646–658.

107. Lange, J. (2021). CliquePercolation: An R package for conducting and visualizing results of the clique percolation network community detection algorithm. J. Open Source Softw. *6*, 3210.

108. Alexa, A.R. (2024). topGO: Enrichment analysis for gene ontology. Bioconductor. https://bioconductor.org/packages/topGO.

109. Singh, A., and Saint-Antoine, M. (2022). Probing transient memory of cellular states using single-cell lineages. Front. Microbiol. *13*, 1050516.

110. Singh, A., and Hespanha, J.P. (2010). Stochastic hybrid systems for studying biochemical processes. Philos. Trans. A Math. Phys. Eng. Sci. *368*, 4995–5011.

111. Krueger, F., and Andrews, S.R. (2011). Bismark: a flexible aligner and methylation caller for Bisulfite-Seq applications. Bioinformatics *27*, 1571–1572.

112. Lawrence, M., Huber, W., Pagès, H., Aboyoun, P., Carlson, M., Gentleman, R., Morgan, M.T., and Carey, V.J. (2013). Software for computing and annotating genomic ranges. PLoS Comput. Biol. *9*, e1003118.

113. CHO-Epigenome | Downloads. https://cho-epigenome.boku.ac.at/download.html.

114. Quinlan, A.R., and Hall, I.M. (2010). BEDTools: a flexible suite of utilities for comparing genomic features. Bioinforma. Oxf. Engl. *26*, 841–842.

115. Langmead, B., and Salzberg, S.L. (2012). Fast gapped-read alignment with Bowtie 2. Nat. Methods *9*, 357–359.

116. Ernst, J., and Kellis, M. (2012). ChromHMM: automating chromatin-state discovery and characterization. Nat. Methods *9*, 215–216.

117. Love, M.I., Huber, W., and Anders, S. (2014). Moderated estimation of fold change and dispersion for RNA-seq data with DESeq2. Genome Biol. *15*, 550.

118. Zhu, X.-F., Li, W., Ma, J.Y., Shao, N., Zhang, Y.J., Liu, R.M., Wu, W.B., Lin, Y., and Wang, S.M. (2015). Knockdown of heme oxygenase-1 promotes apoptosis and autophagy and enhances the cytotoxicity of doxorubicin in breast cancer cells. Oncol. Lett. *10*, 2974–2980.

119. Funes, S.C., Rios, M., Fernández-Fierro, A., Covián, C., Bueno, S.M., Riedel, C.A., Mackern-Oberti, J.P., and Kalergis, A.M. (2020). Naturally derived heme-oxygenase 1 inducers and their therapeutic application to immune-mediated diseases. Front. Immunol. *11*, 1467.

120. Orellana, C.A., Marcellin, E., Palfreyman, R.W., Munro, T.P., Gray, P.P., and Nielsen, L.K. (2018). RNA-seq highlights high clonal variation in monoclonal antibody producing CHO cells. Biotechnol. J. *13*, 1700231.

121. Pavón, M.A., Arroyo-Solera, I., Téllez-Gabriel, M., León, X., Virós, D., López, M., Gallardo, A., Céspedes, M.V., Casanova, I., López-Pousa, A., et al. (2015). Enhanced cell migration and apoptosis resistance may underlie the association between high SERPINE1 expression and poor outcome in head and neck carcinoma patients. Oncotarget *6*, 29016–29033.

122. Zhang, Q., Lei, L., and Jing, D. (2020). Knockdown of SERPINE1 reverses resistance of triple-negative breast cancer to paclitaxel via suppression of VEGFA. Oncol. Rep. *44*, 1875–1884.

123. Pavón, M.A., Arroyo-Solera, I., Céspedes, M.V., Casanova, I., León, X., and Mangues, R. (2016). uPA/uPAR and SERPINE1 in head and neck cancer: role in tumor resistance, metastasis, prognosis and therapy. Oncotarget *7*, 57351–57366.

124. Zhou, L., Cheng, L., He, Y., Gu, Y., Wang, Y., and Wang, C. (2016). Association of gene polymorphisms of FV, FII, MTHFR, SERPINE1, CTLA4, IL10, and TNFalpha with pre-eclampsia in Chinese women. Inflamm. Res. *65*, 717–724.

125. Ma, L., and Chung, W.K. (2014). Quantitative analysis of copy number variants based on real-time lightcycler PCR. Curr. Protoc. Hum. Genet. *80*, 7.21.1–7.21.8.

126. Shahid, M., Hermes, E.L., Chandra, D., Tauseef, M., Siddiqui, M.R., Faridi, M.H., and Wu, M.X. (2018). Emerging potential of immediate early response gene X-1 in cardiovascular and metabolic diseases. J. Am. Heart Assoc. *7*, e009261.

127. Zhou, Q., Hahn, J.K., Neupane, B., Aidery, P., Labeit, S., Gawaz, M., and Gramlich, M. (2017). Dysregulated IER3 expression is associated with enhanced apoptosis in titin-based dilated cardiomyopathy. Int. J. Mol. Sci. *18*, 723.

128. Arlt, A., and Schäfer, H. (2011). Role of the immediate early response 3 (IER3) gene in cellular stress response, inflammation and tumorigenesis. Eur. J. Cell Biol. *90*, 545–552.

129. Zhang, J., Wang, Y., Li, G., Yu, H., and Xie, X. (2014). Down-regulation of nicotinamide N-methyltransferase induces apoptosis in human breast cancer cells via the mitochondria-mediated pathway. PLoS One *9*, e89202.

130. Xie, X., Yu, H., Wang, Y., Zhou, Y., Li, G., Ruan, Z., Li, F., Wang, X., Liu, H., and Zhang, J. (2014). Nicotinamide N-methyltransferase enhances the capacity of tumorigenesis associated with the promotion of cell cycle progression in human colorectal cancer cells. Arch. Biochem. Biophys. *564*, 52–66.

131. Somerville, T.D.D., Xu, Y., Miyabayashi, K., Tiriac, H., Cleary, C.R., Maia-Silva, D., Milazzo, J.P., Tuveson, D.A., and Vakoc, C.R. (2018). TP63-mediated enhancer reprogramming drives the squamous subtype of pancreatic ductal adenocarcinoma. Cell Rep. *25*, 1741–1755.e7.

132. Melino, G. (2011). p63 is a suppressor of tumorigenesis and metastasis interacting with mutant p53. Cell Death Differ. *18*, 1487–1499.

133. Chen, K., Li, D., Li, H., Li, B., Li, J., Huang, L., Li, R., Xu, X., Jiang, L., Jiang, C., et al. (2017). Genetic analysis of heterogeneous sub-clones in recombinant Chinese hamster ovary cells. Appl. Microbiol. Biotechnol. *101*, 5785–5797.

134. Chevallier, V., Schoof, E.M., Malphettes, L., Andersen, M.R., and Workman, C.T. (2020). Characterization of glutathione proteome in CHO cells and its relationship with productivity and cholesterol synthesis. Biotechnol. Bioeng. *117*, 3448–3458.

135. Ku, H.-C., and Cheng, C.-F. (2020). Master regulator activating transcription factor 3 (ATF3) in metabolic homeostasis and cancer. Front. Endocrinol. *11*, 556.

STAR★METHODS

KEY RESOURCES TABLE

REAGENT or RESOURCE	SOURCE	IDENTIFIER
Experimental models: Cell lines		
CHOZN® GS$^{-/-}$ ZFN, Clone 23 Cells (*C.griseus*)	MilliporeSigma	N/A
Antibodies		
Silu^{TM}mab Stable-Isotope Labeled Universal Monoclonal Antibody Standard	Sigma-Aldrich	MSQC3-100UG
Oligonucleotides		
Stellaris® RNA FISH Probes	LGC, Biosearch Technologies	N/A
Chemicals, peptides, and recombinant proteins		
EX-CELL® CD CHO Fusion Medium	Sigma-Aldrich	14365C-1000ML
EX-CELL® CHO Cloning Media	Sigma-Aldrich	C6366-500ML
Fetal Bovine Serum	Sigma-Aldrich	F0926-100ML
EX-CELL® Advanced CHO Fed-batch Medium	Sigma-Aldrich	14366C-1000ML
EX-CELL® Advanced CHO Feed 1 (without glucose)	Sigma-Aldrich	24368C-1L
D-(+)-Glucose Solution	Sigma-Aldrich	G8769-100ML
RNAlater RNA Preservation Solution	Sigma-Aldrich	R0901-100ML
Stellaris® RNA FISH Hybridization Buffer	LGC, Biosearch Technologies	SMF-HB1-10
Stellaris® RNA FISH Wash Buffer A	LGC, Biosearch Technologies	SMF-WA1-60
Stellaris® RNA FISH Wash Buffer B	LGC, Biosearch Technologies	SMF-WB1-20
VECTASHIELD® PLUS Antifade Mounting Medium	Vector Labratories	H-1900-2
Ammonium chloride	VWR	BDH9208-500G
Sodium lactate	Sigma-Aldrich	71718-10G
Sodium chloride	Sigma-Aldrich	S9888-25G
miRNeasy Mini Kit	Qiagen	217084
125-mL Erlenmeyer flasks	Corning	CLS431143
Non-treated 96-well plates	CELLTREAT	229596
18 mm diameter, #1 thickness fibronectin coated coverglass	Neuvitro Corporation	GG-18-Fibronectin
Software and algorithms		
RStudio	https://www.r-project.org/	N/A
ImageJ	https://imagej.net/ij/	N/A
RNA Sequencing and MemorySeq Processing and Analysis Code	https://github.com/SGrissomUDel/CHOCell_MemorySeq	N/A
Deposited data		
RNA Sequencing Data	https://www.ncbi.nlm.nih.gov/geo/query/acc.cgi?acc=GSE232813	GEO: GSE232813
Other		
Minitron incubator	INFORS HT	N/A
Agilent 5200 Fragment Analyzer	Agilent	N/A
Illumina® HiSeq 4000®	Illumina	N/A
Stellaris 8 tauSTED/FLIM confocal microscope	Leica Microsystems	N/A
DeNovix® CellDrop	DeNovix	N/A
Bio-Monolith Protein A, 4.95 × 5.2 mm	Agilent	5069-3639
Agilent 1290 Infinity II Series HPLC System	Agilent	N/A

EXPERIMENTAL MODEL AND STUDY PARTICIPANT DETAILS

Cell lines and culture maintenance

A recombinant CHOZN® GS$^{-/-}$ ZFN, a CHO-K1 subclone with glutamine synthetase (GS) knocked out for glutamine selection, provided by MilliporeSigma was used for this work. This subclone, referred to as CHOZN® GS$^{-/-}$ Clone 23, expressed a monoclonal antibody and GS for selection. These cells were grown in EX-CELL® CD CHO Fusion Medium (Sigma-Aldrich, St. Louis, MO), deficient in glutamine and seeded and passaged in 125-mL Erlenmeyer flasks (Corning, Corning, NY) with a working volume of 25 mL. The cells were cultured in a Minitron incubator (INFORS HT, Bottmingen, Switzerland) at 37°C, 5% CO_2, 80% relative humidity, and shaking at 100 rpm with passages every 3 days at a cell density of 0.5×10^6 cells/mL.

METHOD DETAILS

Single cell limited dilution cloning

Single cell limited dilution cloning (LDC) was used to isolate monoclonal pools for MemorySeq. To assist outgrowth with vital growth factors and nutrients during LDC, conditioned media was produced by harvesting sufficient cells in a 25 mL flask to achieve a seeding density of 1.0×10^6 cells/mL. The cell culture media was harvested 24 hours post-initiation by centrifuging the culture medium at $200 \times g$ for 5 minutes and sterile filtering the media through a 0.22 μ m syringe filter. Conditioned media was stored at 4°C for no longer than seven days.

24 hours before starting LDC, a stock culture was seeded at 1.0×10^6 cells/mL. Sufficient cell culture volume was collected and serially diluted to obtain a final concentration of 2.5 cells/mL in an 80%/20% mix of EX-CELL® CHO Cloning Media (Sigma-Aldrich, St. Louis, MO) and conditioned media. Six non-treated 96-well plates (CELLTREAT, Pepperell, MA) were seeded with 200 μ L of the mix for an average of 0.5 cells/well. Plates incubated under static conditions at 37°C, 5% CO_2, and 80% relative humidity and were undisturbed for 7 days. Afterwards, plates were inspected using a light optical microscope and wells with outgrowth originating from a single location were noted as single cell pools while those with no outgrowth or outgrowth from multiple places were discarded. The plates were fed an additional 20 μ L of EX-CELL® CHO Cloning Media to supplement growth and maintain volume after evaporation. After 3 weeks, single cell colonies reached roughly 100,000 cells or 80% confluency.

RNA extraction and sequencing

Cell samples were collected either from LDC plates, standard passage flasks, or from fed-batch flasks. For MemorySeq RNA extraction, $8 \times 10^4 - 12 \times 10^4$ cells were collected for extraction and for fed-batch flasks, 2.5×10^6 cells were used for extraction. RNA was extracted using the miRNeasy Mini Kit (Qiagen, Germantown, MD) following manufacturer's protocol. All RNA samples were run on the Agilent 5200 Fragment Analyzer (Agilent, Santa Clara, CA) to verify RNA quality prior to submission for sequencing. Samples with an RIN $\geq$ 6.0 and at least 100 ng of high quality RNA were sent for sequencing. For MemorySeq, the target was 40 RNAseq samples for both MemorySeq monoclonal samples and noise control samples, but after quality selection only 38 samples and 40 samples remained for MemorySeq samples and noise control samples respectively. RNAseq samples were submitted to Azenta for RNA selection using poly(A) selection and library preparation. Samples were sequenced on the Illumina® HiSeq 4000® and were sequenced at a coverage of at least 19× and on average 24× with at least uniquely mapped 10 million reads per RNA sequencing library. Sequencing files were returned as FASTQ files and stored online at GEO Series accession number GEO: GSE232813 (See key resources table for publicly deposited reads) along with the converted count tables. Raw FASTQ files were transferred to the University of Delaware Biomix HPC cluster where they were processed through a pipeline consisting of Trim Galore for adapter trimming/quality control, STAR for RNAseq alignment to CriGri-PICR, Samtools for file conversion, and HTSeq to enumerate unique and high-quality mapped reads.[101–105] Gene count tables were transferred to R and processed further depending on the application. The RNA-seq processing pipeline is available at (See key resources table for publicly available code).

smRNA-FISH and imaging

Small molecule RNA fluorescence *in-situ* hybridization (smRNA-FISH) was used to visualize the relationship between cells sharing a common lineage and the maintenance of heritable gene expression states. RNA FISH probes were designed using the Stellaris® Probe Designer software (LGC, Biosearch Technologies, Hoddesdon, United Kingdom) and included 30-48 probes that had length a 20 bp, at least 2 bp of spacing, and either Quasar® 570 or Quasar® 670 fluorescent dyes. These probes were designed to target Hmox1 and Ier3 as identified from MemorySeq. To track the shared lineage of dividing cells, 10,000 CHOZN® GS$^{-/-}$ Clone 23 cells suspended in 90% EX-CELL® CD CHO Fusion Medium/10% FBS were first fixed onto an 18 mm diameter, #1 thickness fibronectin coated coverglass by centrifugation with 30 minute incubation at 37°C. The coverglasses were incubated at statically at 37°C, 5% CO_2, and 80% relative humidity for 7 days or until 50%–60% confluency after unattached cells were gently washed off.

Multiplex smRNA-FISH was achieved using the Stellaris® RNA FISH reagents (LGC, Biosearch Technologies, Hoddesdon, United Kingdom) according to manufacturer's protocol for adherent cells. Briefly, this involved fixation using 3.7% v/v formaldehyde solution in 1× PBS for 10 minutes and permeabilization using 70% ethanol for storage at 4°C. Before hybridization, coverglasses were washed with a wash buffer containing 10% formamide. Coverglasses were then transferred to a humidity chamber and incubated in a hybridization buffer containing 10% formamide and a Quasar® 570 or Quasar® 670 labeled RNA FISH probe and incubated

for 16 hours. After hybridization, coverglasses were washed with a 10% formamide wash buffer before staining with DAPI. After mounting with Vectashield Mounting Medium, samples were imaged immediately using a Stellaris 8 tauSTED/FLIM confocal microscope (Leica Microsystems, Wetzlar, Germany).

Stress-condition fed-batch

Fed-batch flasks were established to adapt the CHOZN® $GS^{-/-}$ Clone 23 cell line to stress agents characteristic of manufacturing conditions. Fed-batch flasks were seeded from freshly thawed cells after 3 passages to allow recovery. The flasks were seeded at a cell density of 0.5×10^6 cells/mL in 30 mL of EX-CELL® Advanced CHO Fed-batch Medium (Sigma-Aldrich, St. Louis, MO). Starting day 3, EX-CELL® Advanced CHO Feed 1 (Sigma-Aldrich, St. Louis, MO) was fed at 5% of the total volume every other day and D-(+)-glucose solution was fed to maintain a concentration of 4 g/L of glucose starting day 4. Cell viability and cell density was measured daily using the DeNovix® CellDrop (DeNovix, Wilmington, DE). Supernatant and cell pellets were collected every other day starting day 1 and cell samples were stored in RNAlater stabilization solution (ThermoFisher Scientific, Waltham, MA) after washing with 1× PBS. Fed-batch was carried out until all flasks fell below 70% cell viability. Ammonium chloride (VWR, Radnor, PA), sodium lactate (Sigma-Aldrich, St. Louis, MO), and sodium chloride (Sigma-Aldrich, St. Louis, MO) were all spiked in at the beginning of fed-batch at varying concentrations to simulate stress during fed-batch production. Analysis of variance (ANOVA) and two-sample t-test assuming equal variance were used for determining significance between conditions.

QUANTIFICATION AND STATISTICAL ANALYSIS

MemorySeq processing

For the computational analysis of MemorySeq samples and noise control samples, the raw count for each gene was converted to transcripts per million (TPM). The genes were filtered out such that only protein-coding genes and TPM $\geq$ 2.5 were included in the dataset. Metrics of variation, including average, standard deviation, coefficient of variation, skewness, and kurtosis were all calculated for each gene in each dataset. Heritable gene expression states were defined as genes with TPM $\geq$ 2.5 and in the 98th percentile for residuals from the Poisson regression fit. Bootstrapped 95% confidence intervals were generated by sampling with replacement of from all MemorySeq or noise control samples until 10,000 bootstrap samples were generated. The bounds of the interval were identified by ordering all CV in ascending order and identifying the value for which 2.5% of the CV values were above and below that point. Asymptotic tests of CV equality were generated using the cvequality package in R.[106] Any gene expression states in the noise control that exceeded the residual cutoff were removed from the heritable pool. This yielded 199 unique heritable gene expression states. To understand how heritable gene expression states co-fluctuate with each other, a correlation matrix was generated using pairwise Pearson correlation coefficients. The resulting matrix, containing all unique significantly heritable gene expression states, had dimensions of 199 genes x 199 genes. Computational analysis and MemorySeq processing tools are available at (See key resources table for publicly available code, Data S1 and S2).

Using the Pearson correlation coefficients matrix for all significantly heritable gene expression state, network communities were generated using a *k*-clique percolation method (*k*-CPM) using the CliquePercolation (0.3.0) package in R.[107] This algorithm detects communities by assigning each gene as an independent node and each node is connected to each other by edges defined as the correlation in the undirected and weighted Pearson correlation matrix. There are two adjustable parameters when generating the network communities. The first is *I*, which defines the intensity threshold or the absolute value of the edge threshold required to connect two nodes. The other is *k*, which defines the minimum number of fully connected nodes to form a *k*-clique. A *k*-clique community then contains all adjacent *k*-cliques that share *k*-1 nodes. A value of *k*=4 was used based on prior *k*-CPM for similar analyses while *I* was varied from 0.6 to 0.98 in order to find the optimal threshold.[48,49] Adjusting *I* changes the size of each *k*-clique community, the number of communities, and the number of isolated nodes. Optimization of *I* can be achieved by tuning *I* such that the ratio of the largest to the second largest community is roughly two and/or maximizing variance after excluding the largest community, where variance, χ, is defined as shown in Equation 1 where N is the total number of communities detected, n_i is the size of the i^{th} community excluding the largest one, and n_j is the size of the j^{th} community excluding the largest community and the i^{th} community.

$$\chi = \sum_{i=1}^{i=N-1} \frac{{n_i}^2}{\left(\sum_{j=1}^{j=N-2} n_j\right)^2} \quad \text{(Equation 1)}$$

Gene ontology (GO) enrichment analysis, a method used to detect the over-representation of certain gene product attributes within a group of genes, was used to assign enriched biological processes to each community to further understand the functional similarities of the co-fluctuating gene networks. GO biological processes terms were collected for 13,288 of the 21,386 protein-coding genes for the CriGri-PICR assembly.[101] GO enrichment analysis was completed using the topGO (2.46.0) R package with a minimum node size of 10.[108] The statistical test of significance was conducted using Fisher's exact test with the classic, weighted, and elimination methods to ensure physically significant enrichment was captured with an adjusted p value < 0.05 (See Data S4: GO Enrichment Analysis).

Prediction of heritability lifetime index

Expression states were modeled as either inheriting the bulk average phenotype (OFF) or a rare deviating phenotype (ON). Exponential cell proliferation or growth rate was modelled by k_x (a generation time of $1/k_x$). MemorySeq clonally derived pools were assumed to be in a constant state of exponential growth throughout the duration of the experiment, (from one cell to divide into 100,000 cells), with a consistent proliferation rate k_x. This proliferation rate was also assumed to be constant with respect to whether an individual cell was in the ON or OFF state. The rate of fluctuation or transition from the ON to OFF state was denoted as k_{OFF} while the inverse transition was denoted as k_{ON}. The fraction of cells displaying the rare ON state in the bulk population, f, was defined in Equation 2, or as the ratio of rates of transition. Previous work conducted by Shaffer et al. found f was typically 1% or less in RNA-FISH and internally confirmed by flow-cytometry.[32]

$$f = \frac{k_{ON}}{k_{ON}+k_{OFF}} \quad \text{(Equation 2)}$$

In this fluctuation analysis, any given cell sampled from the bulk population has a probability f of existing in the rare ON state and probability 1-f of existing in the OFF state. The random variables $x(t)$ and $y(t)$ are then defined as the total number of cells in a given sample and time t in the ON and OFF state respectively. The stochastic time evolution of $x(t)$ and $y(t)$ is dictated by proliferation and the generation of new cells that inherit the ON or OFF state and fluctuations by existing cells between the ON and OFF state. The ratio $x(t)/(x(t) + y(t))$ then represents the fraction of cells in the ON state at a given time t. Using the assumption that $f << 1$ and the first two statistical moments of $x(t)$ and $y(t)$, derived using moment dynamics of stochastic systems (see Singh and Hespanha), the CV^2 of the ratio $x(t)/(x(t) + y(t))$ is given in Equation 3, where $T = tk_x$ represents the duration of the experiment normalized to generation count ($T \approx 17$ generations) and $T_{ON} = k_x/k_{OFF}$ represents the average duration of the ON state normalized to generation count[109,110]

$$CV^2 \times f = \frac{2T_{ON}e^{\left(T-\frac{2T}{T_{ON}}\right)} - 2 - T_{ON}}{(2e^T - 1)(T_{ON} - 2)} \quad \text{(Equation 3)}$$

Application of *a priori* knowledge of f by assuming its value to be 0.01, an inverse transformation of Equation 3 can be used to estimate T_{ON} and the lifetime of certain heritable gene states (See Data S3: Heritability Index for Gene States Identified as Heritable).

Epigenome characterization relative to published data

Seven DNA methylation datasets reflecting 100 bp raw bisulfite-converted DNA from CHO-K1 variants cultured in different conditions produced from Feichtinger et al. were aligned to the CriGri PICR genome (run indices NCBI SRA: ERR866448 - NCBI SRA: ERR866454).[8,101] Trimming and alignment pipeline adapted from Hillard et al.[55] This first involves Trim Galore run in paired-end mode with the first 20 base pairs removed to reduce any bias often introduced during bisulfite sequencing.[102] Reads were then aligned using the Bismark package with the –score_min L,0,-0.3, -N 1, -D 20, and -R 30 options.[111] The heritable and non-heritable gene expression states were extracted for either the gene body (including introns and exons) or for the -1000 region relative to the transcription start site using the GenomicRanges package in R.[112] The methylation percentage for CpG islands with at least a coverage of 4 were identified for these two regions.

ChIP-seq data, generated by Feichtinger et al., was aligned and the ChromHMM model built from an adapted method from Hillard et al.[8,55] Three different batch timepoints (Tp5, Tp9, and Tp13) were included to develop the consensus ChromHMM model for the PICR genome and included an IgG negative control, H3K27ac, H3K27me3, H3K4me1, H3K4me3, H3K9me3, and H3K36me3.[113] These were downloaded as BAM files before conversion to fastq using BEDTools bamtofastq.[114] They were aligned to the PICR genome using Bowtie2 with the –sensitive-local option.[115] Read alignment files were converted back to coordinate sorted BAM files after removing multi-aligned and mismatched reads using Samtools view with the -q 2 option.[104] Using the ChromHMM software, BAM files were binarized using BinarizeBam to become compatible with LearnModel.[116] The Eleven-state hidden Markov model was learned on the filtered reads with a maximum of 300 iterations to assign a biologically meaningful chromatin states to characteristic histone marks. Regions of the scaffolds with inconsistent state declarations across timepoints were considered "non-consensus." Similarly, GenomicRanges in R was used to identify differential chromatin state occupancy between heritable and non-heritable gene expression states[112]

Stress-condition fed-batch analysis

Transcriptomic analysis was conducted on cell-samples by first extracting RNA, submitting for sequencing, and processing the results as described earlier. They were sequenced at a coverage of at least 65× and on average 75× with at least 35 million uniquely mapped reads per RNA sequencing library. Gene count tables were transferred to R and differential gene expression analysis (DGEA) was conducted using the DESeq2 (1.34.0) package.[117] A $\log_2$ fold change (L2FC) threshold of 0.58 or a 1.5-fold change and a Bejamini-Hochberg adjusted p-value or false discovery rarte (FDR) of 0.05 defined genes with significant differential expression. The intersection of differentially expressed genes and heritable gene expression states was used in GO enrichment analysis to find significantly overrepresented biological processes (See Data S4: GO Enrichment Analysis).